

Fine-Grained Trajectory Optimization of Multiple UAVs for Efficient Data Gathering from WSNs

Chuanwen Luo, Meghana N. Satpute^{id}, Deying Li^{id}, Yongcai Wang^{id}, *Member, IEEE*, Wenping Chen, and Weili Wu, *Senior Member, IEEE*

Abstract—The increasing availability of autonomous small-size Unmanned Aerial Vehicles (UAVs) has provided a promising way for data gathering from Wireless Sensor Networks (WSNs) with the advantages of high mobility, flexibility, and good speed. However, few works considered the situations that multiple UAVs are collaboratively used and the fine-grained trajectory plans of multiple UAVs are devised for collecting data from network including detailed traveling and hovering plans of them in the continuous space. In this paper, we investigate the problem of the Fine-grained Trajectory Plan for multi-UAVs (FTP), in which m UAVs are used to collect data from a given WSN, where $m \geq 1$. The problem entails not only to find the flight paths of multiple UAVs but also to design the detailed hovering and traveling plans on their paths for efficient data gathering from WSN. The objective of the problem is to minimize the maximum flight time of UAVs such that all sensory data of WSN is collected by the UAVs and transported to the base station. We first propose a mathematical model of the FTP problem and prove that the problem is NP-hard. To solve the FTP problem, we first study a special case of the FTP problem when $m = 1$, called FTP with Single UAV (FTPS) problem. Then we propose a constant-factor approximation algorithm for the FTPS problem. Based on the FTPS problem, an approximation algorithm for the general version of the FTP problem when $m > 1$ is further proposed, which can guarantee a constant factor of the optimal solution. Afterwards, the proposed algorithms are verified by extensive simulations.

Index Terms—Unmanned Aerial Vehicle, Wireless Sensor Network, data gathering, mobile collector, trajectory optimization.

I. INTRODUCTION

IN WIRELESS Sensor Networks (WSNs), sensors with limited battery resources are deployed on the detection areas to monitor the environment and their sensory data

Manuscript received January 9, 2020; revised August 3, 2020 and September 24, 2020; accepted September 25, 2020; approved by IEEE/ACM TRANSACTIONS ON NETWORKING Editor C. F. Chiasserini. Date of publication October 9, 2020; date of current version February 17, 2021. This work was supported in part by the National Natural Science Foundation of China under Grant 12071478, Grant 11671400, Grant 61972404, and Grant 61672524; and in part by the National Science Foundation (NSF) under Grant 1907472. (*Corresponding author: Deying Li.*)

Chuanwen Luo is with the School of Information Science and Technology, Beijing Forestry University, Beijing 100083, China, also with the Engineering Research Center for Forestry-Oriented Intelligent Information Processing, National Forestry and Grassland Administration, Beijing 100083, China, and also with the School of Information, Renmin University of China, Beijing 100872, China (e-mail: chuanwenluo@bjfu.edu.cn).

Meghana N. Satpute and Weili Wu are with the Department of Computer Science, The University of Texas at Dallas, Richardson, TX 75080 USA (e-mail: mns086000@utdallas.edu; weiliwu@utdallas.edu).

Deying Li, Yongcai Wang, and Wenping Chen are with the School of Information, Renmin University of China, Beijing 100872, China (e-mail: deyingli@ruc.edu.cn; ycw@ruc.edu.cn; chenwenping@ruc.edu.cn).

Digital Object Identifier 10.1109/TNET.2020.3027555

needs to be collected to the base station [1], [2]. In the past decades, a huge amount of architectures tailored to Low Power Wide Area Networks (LPWANs), such as LORAWAN, SIGFOX, NB-IOT and LTE-M, have been prosperous in both urban and remote areas, in which the installation of few gateways over the territory allows to gather data even from sensors that are placed at different miles from the gateways. However, one of the prominent features, and subsequently one of the main problems with these architectures is that they rely heavily on infrastructure. Infrastructure-based networks tend to be susceptible to major damage by natural disasters and other catastrophic situations, such as hurricane, earthquake, volcanic, etc [3]. Therefore, in these situations, the fast and effective data collection methods from WSNs can effectively reduce the losses of lives and property. Due to the complexity of terrain and environment of the detection areas, data collection via multi-hop communication or ground mobile collectors faces many practical challenges. For examples, multi-hop communication makes the energy of sensors around the base station deplete much faster than others, which shortens the lifetime of the network; and the obstacles in the detection areas may inhibit ground mobile collectors to gather data from sensors, since the sensors are generally deployed in complex ground environments, especially in rugged and hilly terrain. The fast development of Unmanned Aerial Vehicles (UAVs) is providing an emerging solution to these challenging tasks due to their high maneuverability, good speed, flexibility, and increasing carrying capacity [4], [5]. The architecture of the UAV-based WSN is shown in Fig.1, in which sensors are deployed in the monitoring area to detect environment information. UAVs act as mobile collectors to gather data generated by sensors from WSN and transmit the data to the base station for data forwarding. Then the received data by the base station is transmitted to the users through the Internet or Satellite for further computational analysis to determine the appropriate response mechanism.

In recent years, there are many researches which proposed various problems and algorithms for the trajectory optimization of UAVs to effectively collect sensory data from WSNs, such as [6]–[9]. In [6], Kim *et al.* investigated the trajectory optimization problem of multiple UAVs, in which UAVs are employed to jointly collect sensory data from a given set of sensors to minimize the task completion time. However, their models of the problems are defined on the two-dimensional plane without considering flight altitude and data transmission expenditure for data gathering from sensors. In [7], Gong *et al.*

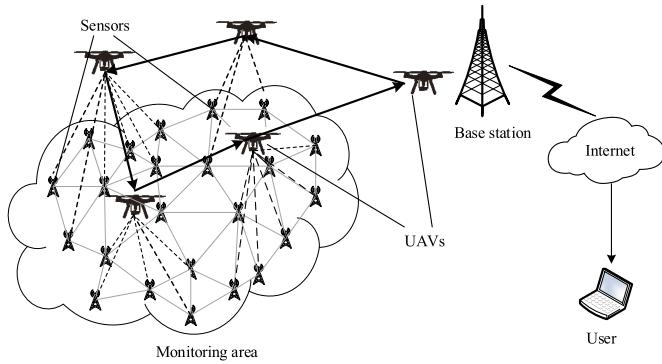


Fig. 1. The architecture of the UAV-based WSN.

studied the flight time minimization problem of UAV for data collection from WSN, in which they considered the case that the UAV can collect data from sensors during either cruising or hovering. However, they only gave the solution for the situation where the single UAV gathers sensory data from sensors located on a line. In [8], Ghorbel *et al.* proposed an energy-efficient method to minimize the energy consumption of both the UAV and the sensors while accomplishing a tour to collect data from WSN. They took into account the total consumption of both traveling and hovering for data collection. But they only considered data gathering on the fixed hovering points and ignored the situation where the UAV can collect data during flight. In [9], Luo *et al.* investigated the Transportation and Communication Latency Optimization (TCLO) problem, which is to find the optimal flight plan of UAV such that all sensing data carried by sensors is collected by the UAV and transported to the base station, while the data collection latency of UAV is minimized. They considered the situation where single UAV collects data from sensors during flight, but they ignored the circumstance in which multiple UAVs are collaboratively used to gather sensory data from sensors.

To overcome the shortcomings of the above research works, in this paper, we focus on fine-grained trajectory plans of multiple UAVs in three-dimensional free space. It optimizes not only the paths of UAVs but also detailed hovering and traveling plans of UAVs for efficient data gathering from WSN. We aim at optimizing the flight trajectories of multiple UAVs such that all sensing data generated by sensors are transported to the base station and the maximum flight time of UAVs is minimized. The contributions of this paper are as below.

(1) We propose a multi-UAVs data gathering model in WSNs, which is called Fine-grained Trajectory Plan for multi-UAVs (m -UAVs) (FTP) problem, where $m \geq 1$. It is to find the optimal fine-grained flight plans of multiple UAVs to gather data from WSN such that the maximum time consumption of UAVs is minimized. Then we give a mathematical model for the FTP problem and prove that it is NP-hard.

(2) We first study a special case of the FTP problem when $m = 1$, called FTP with Single UAV (FTPS), in which the single UAV is used to complete data gathering tasks from a given WSN. To solve the FTPS problem, we present another problem, namely the Path Plan of Single-UAV (PPS), which is to find a detailed flight plan of the UAV in the data collection area of a sensor. Then we propose an approximation

algorithm to solve the PPS problem. Based on the PPS problem, we devise an approximation algorithm FTPSA with the performance ratio $2 + \epsilon$ for the FTPS problem, where $0 < \epsilon < 1$ is a constant.

(3) We extend the solution for the FTPS problem to the general FTP problem, where $m > 1$, and propose an approximation algorithm FTPM with the performance ratio $3 + \epsilon$ for approximating the optimal solution of the FTP problem, where $0 < \epsilon < 1$ is a constant.

(4) The extensive simulations are presented to verify the effectiveness of the proposed algorithm for the FTP problem.

The remainder of this paper is organized as follows. Section II introduces related works. In Section III, we introduce some models and definitions of the problem. In Section IV, we propose an approximation algorithm for solving the FTPS problem. Section V introduces an approximation algorithm for the FTP problem. Simulations are shown in Section VI. Section VII concludes this paper.

II. RELATED WORKS

In this section, we briefly review the literature related to the trajectory optimization problems of UAVs as collectors for sensory data collection in WSNs. Based on the mobility of collectors, we classify the investigated problems into two different types: trajectory optimization of ground mobile collectors (e.g. robots and vehicles) in two-dimensional plane and trajectory optimization of UAVs in three-dimensional (3D) space.

Trajectory Optimization of Ground Mobile Collectors: In [10], Bhaduria and Isler introduced a path planning problem, called k -DGP, in which multiple robots are used to gather data from stationary devices with wireless communication capabilities in WSN. The objective of the problem is to compute tours of k robots such that all data carried by sensors is collected by robots and the time cost of robots is minimized. In [11], Huang *et al.* investigated the data delivery delay problem in WSNs, in which mobile nodes attached to buses were used to collect data from sensors. The goal of the problem is to route delay sensitive data from sensors to mobile nodes within an allowed latency. In [12], Singh *et al.* proposed a scheme using an unequal fixed grid-based cluster along with a mobile data mule for data collection from the cluster heads in WSN, which could overcome the challenge of the high energy depletion rate in nodes near to the base station to maximize the lifetime of the network. In [13], Kumar and Dash investigated the data collection problem in WSN using a mobile collector, in which the mobile sink efficiently collects data from nearby sensors while moving along a pre-specified path with a constant speed such that the total data collected by the mobile collector is maximized with minimum energy consumption.

Trajectory Optimization of UAVs in 3D Space: In [14], Zeng *et al.* investigated the energy-efficient communication problem for a point-to-point link, in which a UAV is employed to communicate with a ground terminal for a finite time horizon, which is a new design framework that needs to jointly consider the communication throughput and the UAV's propulsion energy consumption. The objective of the problem aims at maximizing the energy efficiency in bits/Joule by optimizing the UAV's trajectory. In [15], Liu *et al.* studied

the problem of UAVs supported data collection for WSN and designed the flight paths for single UAV and multiple UAVs to maximize the capacity of sensors. However, they assumed that the flying paths of UAVs are fixed, which is not in line with the actual situation. In [16], Hamidullah *et al.* investigated the problem of path planning for multiple UAVs to collect data from several RoadSide Units (RSUs), whose goal is to find the time-optimal paths for these UAVs such that they can collectively visit all RSUs and gather all data from RSUs. However, they assumed that the altitude of the RSUs and UAVs are identical, which ignores the impact of flying height of UAVs on path optimization, and they used traditional genetic algorithm and harmony search algorithm to solve the problem. In [17], Liu *et al.* investigated the delay-tolerant sensory data gathering problem in UAV-aided WSNs, in which they consider both the sensor's transmission strategy and UAV's trajectory optimization to minimize the transmission energy consumption while guaranteeing the completed transmission within a given time. They considered the situations that the single UAV is used to collect data from sensors and divided the data transmission deadline into discrete time slots for designing UAV trajectory. In [18], Guo *et al.* studied jointly optimizing the UAV's time allocation between recharging and service, flight trajectory and transmit power allocation to maximize the minimum average rate among all ground users, in which the UAV can be recharged periodically at a fixed depot before providing communication service to ground users. In [19], Lee and Yu proposed the path planning optimization of rechargeable solar-powered UAV based on the gravitational potential energy to expand flight time without energy consumption. In [20], Natalizio *et al.* introduced a novel trajectory planning problem for multiple UAVs that takes into account time and capacity constraints, such as airborne energy and limited computational resources. They solved these problem by leveraging the deployment of training and recharging areas (TRA) in the smart cities for providing services of securely recharging, updating and reconfiguration for UAVs. Then the 3D trajectory planning problem of UAVs moving through TRA was investigated by proposing an online approach. However, the method was only validated and tested through simulation without analyzing performance ratio.

In this paper, we investigate the FTP problem which is to optimize the fine-grained trajectories of multiple UAVs for efficient sensory data gathering from WSNs in 3D free space. It not only can overcome the challenges of data collection with ground mobile collectors such as rugged and hilly terrain of detection areas, low speed but also can conquer the shortcomings of UAV trajectory optimization problems in the above researches. Then we propose a constant factor approximation algorithm to solve the FTP problem, which optimizes not only the paths of UAVs but also detailed hovering and traveling plans of UAVs for efficient data gathering from WSN.

III. MODELS AND DEFINITIONS

In this section, we introduce some models and the definitions of the problem.

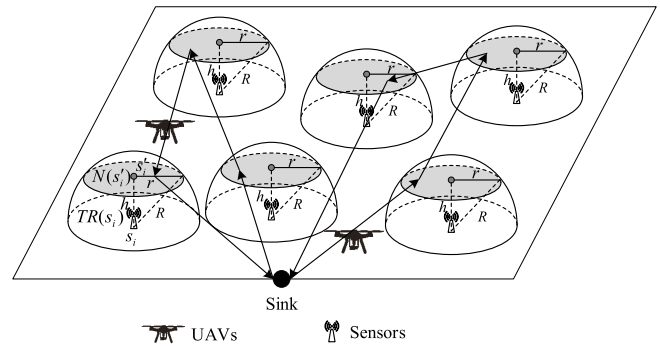


Fig. 2. UAVs act as mobile collectors to gather data from WSN.

A. Network Model

As shown in Fig. 2, we consider a set of n wireless sensors $S = \{s_1, s_2, \dots, s_n\}$ located in the two-dimensional monitoring region $\Omega \subseteq \mathcal{R}^2$ and they have the same three-dimensional transmission range R . Assume that each sensor $s_i \in S$ generates V_i units of sensing data. For each $s_i \in S$, we use $TR(s_i)$ to denote the hemispheric region above the ground which is centered at s_i and whose radius is R . There are several UAVs available to gather sensory data from sensors within the sensors' transmission range. Let $F = \{f_1, f_2, \dots, f_m\}$ denote the set of m UAVs, in which UAVs have the uniform horizontal flight speed v_f , the vertical flight speed v_h and fly at a fixed altitude of h when they fly in horizontal, where $h \leq R$. Let h_0 denote the minimum altitude of UAVs from the ground when they fly in vertical. In practice, v_f and v_h could correspond to the maximum horizontal speed and vertical speed required for minimizing the time consumption of UAVs, respectively and h could correspond to the minimum altitude required for terrain or building avoidance without the need for frequent aircraft ascending and descending. In this paper, we do not consider other higher constraints such as acceleration, weight and steering angle of UAVs. The UAV $f_k \in F$ can collect sensory data from $s_i \in S$ if and only if it is in $TR(s_i)$. All UAVs will start from the stationary base station s_0 when performing their data collection duties and go back to s_0 after finishing their data collection tasks.

In this paper, we use the three-dimensional Cartesian coordinate system XYZ to mark the locations of sensors and UAVs, with all dimensions being measured in meters. Without loss of generality, we assume that all sensors in S are randomly deployed in the first quadrant of the coordinate system and the Z coordinates of them are zero, and let $(x_i, y_i, 0)$ denote the coordinates of sensor $s_i \in S$. For each sensor $s_i \in S$, since the horizontal flight altitude of UAV is h , the horizontal flying data collection area of UAV at flight altitude h in $TR(s_i)$ is a circular area that is the cross-section between $TR(s_i)$ and the plane $Z = h$ in the coordinate system. We use $N(s'_i)$ to represent the circular area which is centered at s'_i and whose radius is $r = \sqrt{R^2 - h^2}$, as the upper gray shaded area shown in Fig.3, where s'_i is the projection of s_i on the $N(s'_i)$ plane, and the X and Y coordinates of s'_i are the same as s_i and its Z coordinate is h . Let $D = \{N(s'_1), N(s'_2), \dots, N(s'_n)\}$. For each sensor $s_i \in S$, since the minimum flying altitude of UAVs is h_0 when they fly in vertical, the data collection area of UAV

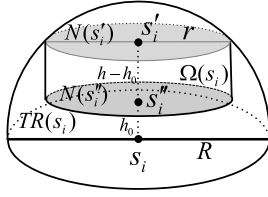


Fig. 3. The data collection area $\Omega(s_i)$ is a cylinder whose top and bottom bases are $N(s'_i)$ and $N(s''_i)$ respectively, and its altitude is $h - h_0$.

in $TR(s_i)$ is a cylinder $\Omega(s_i) \subset TR(s_i)$, one of whose bases is $N(s'_i)$, which is formed by moving down the base $N(s'_i)$ for the distance $h - h_0$. Let $N(s''_i)$ denote the other base of $\Omega(s_i)$ which is centered at s''_i and whose radius is also r , where s''_i is the projection of s_i on $N(s''_i)$ and its X and Y coordinates are the same as s_i and its Z coordinate is h_0 , as shown in Fig. 3. That means the UAV can collect data from s_i only when it travels (or hovers) in $\Omega(s_i)$. Let $\Theta = \{\Omega(s_1), \Omega(s_2), \dots, \Omega(s_n)\}$ be the set of the data collection areas of UAVs. For simplicity, we denote $\{x_0, y_0, z_0\}$ as the coordinate of s_0 . If U_k is the flight path of $f_k \in F$, then we use $L(U_k)$ to represent the length of U_k . For any two different points u and w on U_k , we use $P_{u,w}$ to denote the path between them on U_k and (u, w) to represent the line segment for connecting the two points. Let $L(P_{u,w})$ stand for the length of $P_{u,w}$ and $d_{u,w}$ be the Euclidean distance between u and w .

For any pair of sensors $s_i, s_j \in S$, if they are within each other's communication range, then they can communicate with each other. Therefore, the cluster head sensors can be selected by clustering algorithms from sensors in the network and could enable basic data gathering work in WSNs. For this reason, the UAVs can focus on gathering sensing data from cluster head sensors, such as [12], [21]. In this paper, we assume that any two data collection areas $\Omega(s_i) \in \Theta$ and $\Omega(s_j) \in \Theta$ are disjoint from each other.

B. Communication Model

For each $f_k \in F$, it can gather data from sensor $s_i \in S$ only when it is in $\Omega(s_i)$. As the data transmission rate from s_i to f_k changes with the varying transmission distance under signal path loss model, in this paper, we employ the LOS ground-to-air channel model between UAVs and sensors with path loss exponent $2 \leq \alpha < 4$ that was adopted by [7], [14]. Therefore, the data transmission rate from s_i to f_k can be expressed as

$$C_{ik} = \frac{1}{2} W \log_2 \left(1 + \frac{\beta_0 P}{\sigma^2 d_{s_i, f_k}^\alpha} \right) = \frac{1}{2} W \log_2 \left(1 + \frac{\gamma_0}{d_{s_i, f_k}^\alpha} \right), \quad (1)$$

where d_{s_i, f_k} is the Euclidean distance between s_i and f_k , W represents the channel bandwidth, β_0 denotes the channel power at the reference distance $d_0 = 1\text{m}$, σ^2 is the Gaussian noise power at the UAVs, and $\gamma_0 = \frac{\beta_0 P}{\sigma^2}$ denotes the reference signal-to-noise ratio (SNR) at the reference distance $d_0 = 1\text{m}$.

C. Definition of the Problem

For each $f_k \in F$, let U_k represent the flight tour of f_k where U_k is composed of the horizontal flight path U_k^f and vertical flight path U_k^h , i.e., $U_k = U_k^f \cup U_k^h$. We use H_k to denote the set of hovering points of f_k on U_k and T_k to be the set of hovering

times of f_k at the hovering points in H_k . For any hovering point $HP_{s_i}^k \in H_k$ of f_k in $\Omega(s_i)$, there exists a corresponding hovering time $t_{s_i}^k \in T_k$. Suppose $\Phi(U, H, T)$ is a feasible flight plan of m UAVs such that all sensory data of sensors can be collected by m UAVs and transported to the base station, in which $U = \{U_1, U_2, \dots, U_m\}$, $H = \{H_1, H_2, \dots, H_m\}$ and $T = \{T_1, T_2, \dots, T_m\}$. We use $\phi(U_k, H_k, T_k)$ to denote the flight plan of f_k and $E_\phi^k = L(U_k^f)/v_f + L(U_k^h)/v_h + \sum_{t_{s_i}^k \in T_k} t_{s_i}^k$ to represent the time cost of f_k when its flight plan $\phi(U_k, H_k, T_k)$ has been determined. In this paper, we aim at finding an optimal flight plan $\Phi(U, H, T)$ of m UAVs such that the maximum time consumption $E_\Phi = \max\{E_\phi^k | f_k \in F\}$ is minimized.

We refer to the problem as a Fine-grained Trajectory Plan for multi-UAVs (FTP), whose detailed definition is shown as follows.

Definition 1 FTP: Given a set $S = \{s_1, s_2, \dots, s_n\}$ of n sensors in which each sensor s_i has V_i units of sensing data, a set of data collection areas $\Theta = \{\Omega(s_1), \Omega(s_2), \dots, \Omega(s_n)\}$, a set of disks $D = \{N(s'_1), N(s'_2), \dots, N(s'_n)\}$, a set $F = \{f_1, f_2, \dots, f_m\}$ of m UAVs in which all UAVs have uniform horizontal flight speed v_f , vertical flight speed v_h , flight altitude h for horizontal flying, the minimum vertical flight altitude h_0 and the same initial location s_0 , the Fine-grained Trajectory Plan for multi-UAVs (FTP) problem is to find a flight plan $\Phi(U, H, T)$ for m UAVs such that

- (1) each tour $U_k \in U$ starts from and ends at s_0 ,
- (2) each $f_k \in F$ can collect data from s_i when it flies in (or on the border of) $\Omega(s_i)$,
- (3) for each $s_i \in S$, the UAVs can only fly vertically in the area $\Omega(s_i) \setminus N(s'_i)$,
- (4) for each $s_i \in S$, there exists at least a tour $U_k \in U$ passing through $\Omega(s_i)$ and a hovering point $HP_{s_i}^k \in H_k \cap \Omega(s_i)$ with hovering time $t_{s_i}^k \in T_k$ for some $f_k \in F$ and V_i units of sensing data is transmitted to the base station, and
- (5) $E_\Phi = \max\{E_\phi^k | f_k \in F\}$ is minimized, where $E_\phi^k = L(U_k^f)/v_f + L(U_k^h)/v_h + \sum_{t_{s_i}^k \in T_k} t_{s_i}^k$.

Next, we will introduce the mathematical formulation for the FTP problem. We use q_i^k to denote the projection point of $HP_{s_i}^k$ on $N(s'_i)$. For simplicity, let $V_0 = 0$ denote the amount of data stored by s_0 , $q_0^k = (x_0, y_0, h)$, and $HP_{s_0}^k = s_0$ for each $f_k \in F$. Let V_i^k represent the amount of data collected from s_i by f_k . We define binary variable a_{ijk} as below.

$$a_{ijk} = \begin{cases} 1, & \text{if } f_k \text{ visits } \Omega(s_j) \text{ after } \Omega(s_i), \\ 0, & \text{otherwise.} \end{cases} \quad (2)$$

We can obtain the following mathematical formulation of the FTP problem.

$$\text{Minimize } \max_{1 \leq k \leq m} \sum_{i=0}^n \sum_{\substack{j=0 \\ j \neq i}}^n \left(\frac{d_{q_i^k, q_j^k}}{v_f} + \frac{2 \cdot d_{q_j^k, HP_{s_j}^k}}{v_h} + t_{s_j}^k \right) \cdot a_{ijk} \quad (3)$$

$$\text{s.t. } \sum_{k=1}^m \sum_{j=1}^n a_{0jk} = m \quad (4)$$

$$\sum_{k=1}^m \sum_{i=1}^n a_{i0k} = m \quad (5)$$

$$1 \leq \sum_{k=1}^m \sum_{i=0}^n a_{ijk} \leq m \quad j = 1, 2, \dots, n \quad (6)$$

$$\sum_{i=0}^n a_{ipk} - \sum_{j=0}^n a_{pjk} = 0 \quad k = 1, 2, \dots, m, \quad (7)$$

$$p = 1, 2, \dots, n$$

$$\sum_{i=0}^n \sum_{k=1}^m a_{ijk} \cdot V_j^k = V_j \quad j = 1, 2, \dots, n \quad (8)$$

$$\sum_{s_i \in G} \sum_{s_j \in G} a_{ijk} \leq |G| - 1 \quad \forall G \subset S, G \neq \emptyset, \quad (9)$$

$$k = 1, 2, \dots, m$$

$$a_{ijk} \in \{0, 1\} \quad i = 0, 1, \dots, n \quad (10)$$

$$j = 0, 1, \dots, n, i \neq j, \quad k = 1, 2, \dots, m$$

$$HP_{s_i}^k \in \Omega(s_i) \quad i = 1, 2, \dots, n, k = 1, 2, \dots, m \quad (11)$$

$$q_i^k \in N(s_i') \quad i = 1, 2, \dots, n, k = 1, 2, \dots, m \quad (12)$$

Constraints (4) and (5) express that each UAV goes from the depot s_0 to any data collection area and comes back to the depot. Constraint (6) states that each data collection area should be visited by at least one UAV and at most m UAVs. Constraint (7) is the flow conservation constraint which ensures that once a UAV visits a data collection area, it must also depart from the same area. Constraint (8) ensures that the total amount of data collected from s_j by the visited UAVs is V_j . Constraint (9) ensures connectivity requirement for the solution, i.e., prevents from forming subtours of cardinality G not including the depot s_0 , where G is a subset of S . Constraint (10) defines the domain of the instance. Constraints (11) and (12) limit the position ranges of hovering point $HP_{s_i}^k$ and its projection point q_i^k in each data collection area $\Omega(s_i)$ for any $f_k \in F$.

According to the definition of the FTP problem, the hovering time $t_{s_j}^k$ in the objective formula (3) can be computed as below. If $a_{ijk} = 1$ and $a_{jpk} = 1$, then we compute the intersection point q_b^j between the line segment (q_i^k, q_j^k) and $N(s_i')$ and compute the intersection point q_e^j between the line segment (q_j^k, q_p^k) and $N(s_i')$. Assume that the time of f_k arriving at q_b^j is t_0 . Let $\Gamma = t_0 + \frac{d_{q_b^j, q_i^k}^j}{v_f} + 2 \cdot \frac{d_{q_j^k, HP_{s_i}^k}^j}{v_h} + \frac{d_{q_e^j, q_e^j}^j}{v_f}$ and $t_1 = \frac{d_{q_b^j, q_i^k}^j}{v_f} + \frac{d_{q_j^k, HP_{s_i}^k}^j}{v_h}$. Assume the coordinate of f_k at time $t \in [t_0, \Gamma]$ is $(x^k(t), y^k(t), z^k(t))$. Then, at time $t \in [t_0, \Gamma]$, the data transmission rate from s_j to f_k can be expressed as

$$C_{jk}(t) = \frac{1}{2} W \log_2 \left(1 + \frac{\gamma_0}{d_{s_j, f_k}^\alpha(t)} \right), \quad (13)$$

where $d_{s_j, f_k}(t) = \sqrt{(x^k(t) - x_j)^2 + (y^k(t) - y_j)^2 + (z^k(t) - 0)^2}$. Therefore, the hovering time of f_k at $HP_{s_j}^k$ can be written as

$$t_{s_j}^k = \frac{V_j^k - \int_{t_0}^{\Gamma} C_{jk}(t) dt}{C_{jk}(t_1)}. \quad (14)$$

In the following theorem, we will prove that the FTP problem is NP-hard.

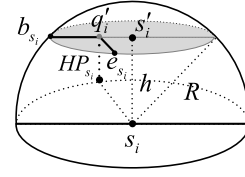


Fig. 4. An example of the flight path U_{s_i} of UAV in $\Omega(s_i)$, which is composed of $U_{s_i}^f$ and $U_{s_i}^h$, where $U_{s_i}^f = (b_{s_i}, q_i^k) \cup (q_i^k, e_{s_i}^k)$ and $U_{s_i}^h = (q_i^k, HP_{s_i}^k) \cup (HP_{s_i}^k, h)$.

Theorem 1: The problem FTP is NP-hard.

Proof: If we set $V_i = 0$ for each sensor $s_i \in S$, $R = 0$, $m = 1$ and $h = h_0 = 0$, then the FTP problem can be reduced to the well-known traveling salesman problem (TSP), which is proved NP-hard [22]. Since a special case of the FTP problem is NP-hard, the FTP problem is also NP-hard. \square

In the FTP problem, a special case is that the single UAV (i.e., $m = 1$) is used for gathering all sensory data from WSN, which is called the FTP with Single UAV (FTPS) problem. Based on Theorem 1, we can find that the FTPS problem is also NP-hard.

IV. ALGORITHM FOR THE FTPS PROBLEM

In this section, we propose an approximation algorithm to solve the FTPS problem. According to the definition of the problem, we can find that the flight plan of UAV consists of two parts. The first is the path for connecting all data collection areas in Θ . The second is the flight plan of UAV in every data collection area $\Omega(s_i)$ for gathering data from $s_i \in S$ including horizontal flight path, vertical flight path and hovering point with corresponding hovering time. Therefore, to solve the FTPS problem, we introduce two other problems, Euclidean TSP with Neighborhoods (TSPN) and Path Plan of Single-UAV (PPS), as shown in Definitions 2 and 3, which can be used as subroutines for the FTPS problem.

Definition 2 TSPN: Given a collection of n disks, $D = \{N(s_1'), N(s_2'), \dots, N(s_n')\}$ where the disks are equal-size and disjoint each other, the TSPN problem aims to find a shortest tour U_f' that visits all disks in D .

The TSPN problem is proved NP-hard, and there exists a $(1+\varepsilon)$ -approximation algorithm for the problem in [23], where $0 < \varepsilon < 1$.

The PPS problem aims at finding an optimal flight plan $\varphi(U_{s_i}, HP_{s_i}, t_{s_i})$ of UAV in the data collection area $\Omega(s_i) \in \Theta$, as shown in Fig. 4, such that V_i units of data carried by s_i is collected by the UAV, where U_{s_i} that consists of the horizontal flight path $U_{s_i}^f$ and vertical flight path $U_{s_i}^h$ is the traveling path of UAV in $\Omega(s_i)$, which starts from a given border point b_{s_i} of $N(s_i')$ and ends at another border point e_{s_i} of $N(s_i')$, and HP_{s_i} represents the hovering point of UAV with hovering time t_{s_i} on U_{s_i} . The objective of the problem is to minimize the time cost $E_\varphi^i = L(U_{s_i}^f)/v_f + L(U_{s_i}^h)/v_h + t_{s_i}$ of UAV. More formally, we formulate this problem as below.

Definition 3 PPS: Given a sensor s_i with V_i units of sensing data, a data collection area $\Omega(s_i)$, a horizontal flying data collection area $N(s_i')$, a border point b_{s_i} of $N(s_i')$ and a UAV with horizontal flight speed v_f , vertical flight speed v_h , horizontal flight altitude h , the minimum vertical flight altitude

Algorithm 1 PPSA

Input: $\Omega(s_i)$, $N(s'_i)$, $b_{s_i} = (x_i^b, y_i^b, h)$, $s'_i = (x_i, y_i, h)$, V_i , r , n , h , h_0 , v_f , v_h , W , γ_0 , M

Output: $\varphi(U_{s_i}, HP_{s_i}, t_{s_i})$

- 1 $\delta = \frac{r}{6n}$, $(p_0, p_1, \dots, p_{6n}) = (b_{s_i}, s'_i)$;
- 2 $\eta = \frac{\delta}{v_f} \cdot v_h$, $\tau = \lceil \frac{h-h_0}{\eta} \rceil$;
- 3 For any $0 \leq t \leq 6n$, $(q_{t,0}, q_{t,1}, \dots, q_{t,\tau}) = (p_t, p'_t)$;
- 4 **for** t from 0 to $6n$ **do**
- 5 **for** l from 0 to τ **do**
- 6 $C_{q_{t,l}} = \frac{1}{2}W \log_2(1 + \frac{\gamma_0}{((r-t)\delta)^2 + (h-l)\eta^2})$;
- 7 **if** $t = 0$ **then**
- 8 1) If $l = 0$, then $V_{t,l} = 0$;
- 9 2) If $1 \leq l < \tau$, then $V_{t,l} = \sum_{j=0}^{l-1} \frac{2\eta}{v_h} \cdot C_{q_{t,j}}$;
- 10 3) If $l = \tau$, then
- 11 $V_{t,l} = \sum_{j=0}^{l-2} \frac{2\eta}{v_h} \cdot C_{q_{t,j}} + \frac{2(h-h_0-(l-1)\eta)}{v_h} \cdot C_{q_{t,l-1}}$;
- 12 **else**
- 13 1) If $l = 0$, then $V_{t,l} = \sum_{k=0}^{t-1} \frac{2\delta}{v_f} \cdot C_{q_{k,0}}$;
- 14 2) If $1 \leq l < \tau$, then
- 15 $V_{t,l} = \sum_{k=0}^{t-1} \frac{2\delta}{v_f} \cdot C_{q_{k,0}} + \sum_{j=0}^{l-1} \frac{2\eta}{v_h} \cdot C_{q_{t,j}}$;
- 16 3) If $l = \tau$, then
- 17 $V_{t,l} = \sum_{k=0}^{t-1} \frac{2\delta}{v_f} \cdot C_{q_{k,0}} + \sum_{j=0}^{l-2} \frac{2\eta}{v_h} \cdot C_{q_{t,j}} + \frac{2(h-h_0-(l-1)\eta)}{v_h} \cdot C_{q_{t,l-1}}$;
- 18 **end**
- 19 **if** $V_{t,l} \geq V_i$ **then**
- 20 $E_{t,l}^i = M$;
- 21 **else**
- 22 $E_{t,l}^i = 2 \cdot (\frac{t\delta}{v_f} + \frac{l\eta}{v_h}) + \frac{V_i - V_{t,l}}{C_{q_{t,l}}}$;
- 23 **end**
- 24 **end**
- 25 **end**
- 26 $E_\varphi^i = \min\{E_{t,l}^i | 0 \leq t \leq 6n, 0 \leq l \leq \tau\}$;
- 27 Return the current t and l , $t_{s_i} = \frac{V_i - V_{t,l}}{C_{q_{t,l}}}$;
- 28 **if** $t = 6n$ **then**
- 29 **if** $l = \tau$ **then**
- 30 $HP_{s_i} = (x_i, y_i, h_0)$
- 31 **else**
- 32 $HP_{s_i} = (x_i, y_i, h - l \cdot \eta)$
- 33 **end**
- 34 **else**
- 35 $\lambda = \frac{t\delta}{r-t\delta}$;
- 36 **if** $l = \tau$ **then**
- 37 $HP_{s_i} = (\frac{x_i^b + \lambda \cdot x_i}{1+\lambda}, \frac{y_i^b + \lambda \cdot y_i}{1+\lambda}, h - h_0)$;
- 38 **else**
- 39 $HP_{s_i} = (\frac{x_i^b + \lambda \cdot x_i}{1+\lambda}, \frac{y_i^b + \lambda \cdot y_i}{1+\lambda}, h - l \cdot \eta)$;
- 40 **end**
- 41 **end**
- 42 $U_{s_i}^f = \bigcup_{0 \leq k < t} (q_{k,0}, q_{k+1,0}) \cup \bigcup_{0 \leq k < t} (q_{k+1,0}, q_{k,0})$;
- 43 $U_{s_i}^h = \bigcup_{0 \leq j < l} (q_{t,j}, q_{t,j+1}) \cup \bigcup_{0 \leq j < l} (q_{t,j+1}, q_{t,j})$;
- 44 $U_{s_i} = U_{s_i}^f \cup U_{s_i}^h$;

h_0 , the Path Plan of Single-UAV (PPS) problem is to find a flight plan $\varphi(U_{s_i}, HP_{s_i}, t_{s_i})$ of UAV in $\Omega(s_i)$ such that

- (1) U_{s_i} starts from b_{s_i} and ends at another border point e_{s_i} (including b_{s_i}) of $N(s'_i)$,
- (2) the UAV can only fly vertically in the area $\Omega(s_i) \setminus N(s'_i)$,
- (3) UAV can gather data from s_i during flying on U_{s_i} and have a hovering point HP_{s_i} with hovering time t_{s_i} on U_{s_i} for gathering the remaining data from s_i ,
- (4) V_i units of sensing data is transmitted to the UAV, and
- (5) $E_\varphi^i = L(U_{s_i}^f)/v_f + L(U_{s_i}^h)/v_h + t_{s_i}$ is minimized.

A. Algorithm for the PPS Problem

In this subsection, we propose an approximation algorithm for solving the PPS problem, which is called PPSA. The objective of the algorithm is to find a flight plan $\varphi(U_{s_i}, HP_{s_i}, t_{s_i})$ of single UAV in $\Omega(s_i)$ such that the total time cost of UAV in $\Omega(s_i)$

$$E_\varphi^i = \frac{L(U_{s_i}^f)}{v_f} + \frac{L(U_{s_i}^h)}{v_h} + t_{s_i} \text{ is minimized,}$$

where $U_{s_i} = U_{s_i}^f \cup U_{s_i}^h$.

Before describing the algorithm, we introduce some terms and notations. Suppose the coordinates of b_{s_i} are (x_1^b, y_1^b, h) . Initially, we divide r into $6n$ equal parts and set $\delta = \frac{r}{6n}$. Let $p_0 = b_{s_i}$ and $p_{6n} = s'_i$. Afterwards, we use $(p_0, p_1, \dots, p_{6n})$ to represent the line segment (b_{s_i}, s'_i) , where p_t is an equidistant point and $d_{p_t, p_{t+1}} = \delta$ for any $0 \leq t \leq 6n - 1$. For arbitrary point $p_t \in \{p_0, p_1, \dots, p_{6n}\}$, there exists a projection p'_t on $N(s'_i)$. Let $\eta = \frac{\delta}{v_f} \cdot v_h$. We divide the line segment (p_t, p'_t) into τ parts, where $\tau = \lceil \frac{h-h_0}{\eta} \rceil$. The first $\tau - 1$ parts are equal and their length is η , and the length of the last part is less than or equal to η . For arbitrary $0 \leq t \leq 6n$, we let $(q_{t,0}, q_{t,1}, \dots, q_{t,\tau})$ denote the line segment (p_t, p'_t) , where $q_{t,l}$ is a breakpoint and $d_{q_{t,l}, q_{t,l+1}} = \eta$ for any $0 \leq l \leq \tau - 2$, and $d_{q_{t,\tau-1}, q_{t,\tau}} = h - h_0 - (\tau - 1) \cdot \eta$. Since the time complexity for calculating integral function grows exponentially, we use the amount of data collected by UAV during hovering at the starting point of a very short path to approximate the amount of data collected by UAV during flying on the path in the same time. For any $0 \leq t < 6n$, we use $\frac{2 \cdot d_{p_t, p_{t+1}}}{v_f} \cdot C_{q_{t,0}}$ to approximate the size of data collected by UAV during flying on the round trip of $(p_t, p_{t+1,0})$, where $C_{q_{t,0}} = \frac{1}{2}W \log_2(1 + \frac{\gamma_0}{((r-t)\delta)^2 + h^2})$ is the data transmission rate of UAV when it hovers at $q_{t,0}$. By taking t , for any $0 \leq l < \tau$, let $\frac{2 \cdot d_{q_{t,l}, q_{t,l+1}}}{v_h} \cdot C_{q_{t,l}}$ approximate the amount of data collected by UAV during flying on the round trip of $(q_{t,l}, q_{t,l+1})$, where $C_{q_{t,l}} = \frac{1}{2}W \log_2(1 + \frac{\gamma_0}{((r-t)\delta)^2 + (h-l)\eta^2})$ represents the data transmission rate of UAV when it hovers at $q_{t,l}$.

The PPSA algorithm consists of four steps as follows.

In the first step, we set $\delta = \frac{r}{6n}$ and $(p_0, p_1, \dots, p_{6n}) = (b_{s_i}, s'_i)$. For each $p_t \in \{p_0, p_1, \dots, p_{6n}\}$, we compute its projection point p'_t on $N(s'_i)$. Let $\eta = \frac{\delta}{v_f} \cdot v_h$ and $\tau = \lceil \frac{h-h_0}{\eta} \rceil$. For arbitrary $0 \leq t \leq 6n$, we set $(q_{t,0}, q_{t,1}, \dots, q_{t,\tau}) = (p_t, p'_t)$. For any $0 \leq l \leq \tau - 2$, let $d_{q_{t,l}, q_{t,l+1}} = \eta$ and $d_{q_{t,\tau-1}, q_{t,\tau}} = h - h_0 - (\tau - 1)\eta$.

In the second step, for any $0 \leq t \leq 6n$ and $0 \leq l \leq \tau$, we compute the time consumption $E_{t,l}^i$ of UAV for gathering V_i units of data from s_i when its hovering point is located at $q_{t,l}$. Let $V_{t,l}$ denote the amount of data collected by UAV during traveling from b_{s_i} to $q_{t,l}$ and from $q_{t,l}$ to b_{s_i} . We compute the value of $V_{t,l}$ in the light of the two cases: $t = 0$ and $0 < t \leq 6n$. Then we compute the time cost $E_{t,l}^i$ of UAV for each of cases as below.

(1) $t = 0$

- If $l = 0$, then $V_{t,l} = 0$.

- If $1 \leq l < \tau$, then $V_{t,l} = \sum_{j=0}^{l-1} \frac{2\eta}{v_h} \cdot C_{q_{t,j}}$.

- If $l = \tau$, then $V_{t,l} = \sum_{j=0}^{l-2} \frac{2\eta}{v_h} \cdot C_{q_{t,j}} + \frac{2(h-h_0-(l-1)\eta)}{v_h} \cdot C_{q_{t,l-1}}$.

(2) $0 < t \leq 6n$

- If $l = 0$, then $V_{t,l} = \sum_{k=0}^{t-1} \frac{2\delta}{v_f} \cdot C_{q_{k,0}}$.

- If $1 \leq l < \tau$, then $V_{t,l} = \sum_{k=0}^{t-1} \frac{2\delta}{v_f} \cdot C_{q_{k,0}} + \sum_{j=0}^{l-1} \frac{2\eta}{v_h} \cdot C_{q_{t,j}}$.

- If $l = \tau$, then $V_{t,l} = \sum_{k=0}^{t-1} \frac{2\delta}{v_f} \cdot C_{q_{k,0}} + \sum_{j=0}^{l-2} \frac{2\eta}{v_h} \cdot C_{q_{t,j}} + \frac{2(h-h_0-(l-1)\eta)}{v_h} \cdot C_{q_{t,l-1}}$.

After obtaining the value of $V_{t,l}$, we compare $V_{t,l}$ with V_i . If $V_{t,l} \geq V_i$, then we set $E_{t,l}^i = M$, otherwise, $E_{t,l}^i = 2 \cdot (\frac{t\delta}{v_f} + \frac{l\eta}{v_h}) + \frac{V_i - V_{t,l}}{C_{q_{t,l}}}$, where M is a very large real number to control the end of the algorithm.

In the third step, the minimum time cost of UAV is computed as $E_\phi^i = \min\{E_{t,l}^i | 0 \leq t \leq 6n, 0 \leq l \leq \tau\}$, and the corresponding t and l are obtained.

In the fourth step, based on the values of t and l , we compute the flight plan $\phi(U_{s_i}, HP_{s_i}, t_{s_i})$ of UAV in the area $\Omega(s_i)$. Firstly, for any $0 \leq t < 6n$, we let $\lambda = \frac{t\delta}{r-t\delta}$ and $\lambda = 0$ for $t = 6n$. Then based on the different values of l obtained from the above processes, we can compute the coordinates of HP_{s_i} with the following cases.

- If $0 \leq l < \tau$, then $HP_{s_i} = (\frac{x_i^h + \lambda \cdot x_i}{1+\lambda}, \frac{y_i^h + \lambda \cdot y_i}{1+\lambda}, h - l \cdot \eta)$.

- If $l = \tau$, then $HP_{s_i} = (\frac{x_i^h + \lambda \cdot x_i}{1+\lambda}, \frac{y_i^h + \lambda \cdot y_i}{1+\lambda}, h - h_0)$.

Based on the coordinates of HP_{s_i} , we compute the traveling path U_{s_i} and of UAV in $\Omega(s_i)$ and its hovering time t_{s_i} on HP_{s_i} , where $U_{s_i} = \bigcup_{0 \leq k < t} (q_{k,0}, q_{k+1,0}) \cup \bigcup_{0 \leq j < l} (q_{t,j}, q_{t,j+1}) \cup \bigcup_{0 \leq k < t} (q_{k+1,0}, q_{k,0}) \cup \bigcup_{0 \leq j < l} (q_{t,j+1}, q_{t,j})$ and $t_{s_i} = \frac{V_i - V_{t,l}}{C_{q_{t,l}}}$.

Note that for any t and l , the line segments $(q_{t,l}, q_{t,l+1})$ and $(q_{t,l+1}, q_{t,l})$ (or $(q_{t,l}, q_{t+1,l})$ and $(q_{t+1,l}, q_{t,l})$) represent the different traveling paths of UAV since the flight directions of UAV on the two paths are different. After executing the above four steps of the PPSA algorithm, a detailed flight plan of UAV $\phi(U_{s_i}, HP_{s_i}, t_{s_i})$ in $\Omega(s_i)$ is obtained. The pseudo-code of the algorithm is shown in Algorithm 1.

Now, we analyze the performance of the PPSA algorithm. Suppose $\phi(U_{s_i}^*, HP_{s_i}^*, t_{s_i}^*)$ is an optimal flight plan of UAV for the PPS problem, where $U_{s_i}^*$ denotes the optimal traveling path of UAV in $\Omega(s_i)$ and $HP_{s_i}^*$ represents the optimal hovering point of UAV with hovering time $t_{s_i}^*$ on $U_{s_i}^*$. Assume $U_{s_i}^*$ is composed of $U_{s_i}^{f*}$ and $U_{s_i}^{h*}$, where $U_{s_i}^{f*}$ and $U_{s_i}^{h*}$ are the horizontal flight path and vertical flight path of UAV in $\Omega(s_i)$, respectively. Let q_i^* denote the

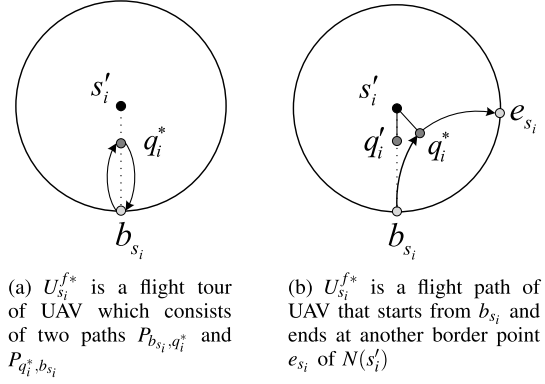


Fig. 5. Two oppositions to the optimal horizontal flight path of UAV.

projection point of $HP_{s_i}^*$ on $N(s_i')$ and $d_{HP_{s_i}^*, q_i^*} = h^*$. We use $E_\phi^{i*} = L(U_{s_i}^{f*})/v_f + L(U_{s_i}^{h*})/v_h + t_{s_i}^*$ to represent the time cost of UAV by executing the flight plan $\phi(U_{s_i}^*, HP_{s_i}^*, t_{s_i}^*)$ and $C_{s_i}^*$ to be the data transmission rate of UAV on $HP_{s_i}^*$.

Lemma 1: The path $U_{s_i}^{f}$ must be a tour which is on the line segment (b_{s_i}, s_i') from b_{s_i} to q_i^* and from q_i^* to b_{s_i} .*

Proof: We use the proof by contradiction. Suppose $U_{s_i}^{f*}$ is not a tour on the line segment (b_{s_i}, s_i') , then two cases should be considered, as shown in Fig. 5. One is that both the starting point and ending point of $U_{s_i}^{f*}$ are b_{s_i} but either of $P_{b_{s_i}, q_i^*}$ and $P_{q_i^*, b_{s_i}}$ or neither of them is on the line (b_{s_i}, s_i') , as shown in Fig. 5(a). The other is that $U_{s_i}^{f*}$ starts from b_{s_i} and ends at another border point e_{s_i} of $N(s_i')$, as shown in Fig. 5(b).

In the first case, we construct a new flight plan $\phi(U_{s_i}, HP_{s_i}, t_{s_i})$ of UAV in $\Omega(s_i)$. Let $HP_{s_i} = HP_{s_i}^*$ be the hovering point of UAV. Let $U_{s_i}^f = (b_{s_i}, q_i^*) \cup (q_i^*, b_{s_i})$ and $U_{s_i}^h = (q_i^*, HP_{s_i}) \cup (HP_{s_i}, q_i^*)$ be the horizontal flight path and vertical flight path of UAV, respectively, and $U_{s_i} = U_{s_i}^f \cup U_{s_i}^h$. Then, we can obtain $L(U_{s_i}^{f*}) > L(U_{s_i}^f)$ and $L(U_{s_i}^{h*}) = L(U_{s_i}^h)$. Assume that the amount of data collected by UAV during flying on $U_{s_i}^h$ is V_i^h and that the average data transmission rate of UAV during traveling on $U_{s_i}^f$ is $\overline{C_{s_i}^f}$. Thus, we can obtain

$$t_{s_i} = \frac{V_i - V_i^h - \frac{L(U_{s_i}^f)}{v_f} \cdot \overline{C_{s_i}^f}}{C_{s_i}^*}, \text{ and } E_\phi^i = \frac{L(U_{s_i}^f)}{v_f} + \frac{L(U_{s_i}^h)}{v_h} + \frac{V_i - V_i^h - \frac{L(U_{s_i}^f)}{v_f} \cdot \overline{C_{s_i}^f}}{C_{s_i}^*}.$$

According to the shapes of the curves $U_{s_i}^{f*}$ and $U_{s_i}^{f*}$, we can find that for each point $p \in U_{s_i}^{f*}$, there exists a point $p' \in U_{s_i}^f$ such that $d_{s_i', p} = d_{s_i', p'}$, which means that the data transmission rate of UAV on p is the same as on p' since $d(s_i, p) = \sqrt{h^2 + d_{s_i', p}^2} = \sqrt{h^2 + d_{s_i', p'}^2} = d(s_i, p')$. Therefore, we can obtain that there exists a part of $U_{s_i}^{f*}$ such that the amount of data collected by UAV during flying on the part is $\frac{L(U_{s_i}^f)}{v_f} \cdot \overline{C_{s_i}^f}$. Suppose the average data transmission of UAV during flying on the path $U_{s_i}^{f*} \setminus U_{s_i}^f$ is $\overline{C_{s_i}^*}$. Since $\overline{C_{s_i}^*} < C_{s_i}^*$, we can obtain

$$\begin{aligned} E_\phi^{i*} &= \frac{V_i - V_i^h - \frac{L(U_{s_i}^f)}{v_f} \cdot \overline{C_{s_i}^f} - \frac{L(U_{s_i}^{f*}) - L(U_{s_i}^f)}{v_f} \cdot \overline{C_{s_i}^*}}{C_{s_i}^*} + \frac{L(U_{s_i}^{f*})}{v_f} + \frac{L(U_{s_i}^{h*})}{v_h} \\ &= E_\phi^i + \frac{L(U_{s_i}^{f*}) - L(U_{s_i}^f)}{v_f} - \frac{L(U_{s_i}^{f*}) - L(U_{s_i}^f)}{v_f} \cdot \frac{\overline{C_{s_i}^*}}{C_{s_i}^*} > E_\phi^i, \end{aligned}$$

which is contradiction to the assumption that E_φ^{i*} is an optimal solution.

In the second case, we construct another new flight plan $\varphi(U_{s_i}, HP_{s_i}, t_{s_i})$ of UAV. We first connect q_i^* with s_i' to obtain the line segment (q_i^*, s_i') . Then we select a point q_i' on the line segment (b_{s_i}, s_i') such that $d_{q_i', s_i'} = d_{q_i^*, s_i'}$, as shown in Fig. 5(b). Let q_i'' represent the projection point of q_i' on $N(s_i')$. We use $p_i' \in (q_i', q_i'')$ to be the hovering point HP_{s_i} of UAV in $\Omega(s_i)$, where $d_{q_i', p_i'} = h^*$. We can obtain that the data transmission rate of UAV at HP_{s_i} is the same as $HP_{s_i}^*$ since $d_{HP_{s_i}, s_i} = \sqrt{(h-h^*)^2 + (r-d_{q_i', s_i'})^2} = d_{HP_{s_i}^*, s_i}$. Afterwards, we let $U_{s_i}^f = (b_{s_i}, q_i') \cup (q_i', b_{s_i})$ and $U_{s_i}^h = (q_i', HP_{s_i}) \cup (HP_{s_i}, q_i')$ be the horizontal flight path and vertical flight path of UAV, respectively. Therefore, we have $L(U_{s_i}^f) > L(U_{s_i}^f)$ and $L(U_{s_i}^h) = L(U_{s_i}^h)$. According to the shapes of the curves $U_{s_i}^f$ and $U_{s_i}^h$, we can obtain that for each point $p \in (b_{s_i}, q_i')$ (or $p \in (q_i', b_{s_i})$), there exists a point $p' \in P_{b_{s_i}, q_i'}$ (or $p' \in P_{q_i', b_{s_i}}$) such that $d_{s_i', p} = d_{s_i', p'}$, which means that the data transmission rate of UAV on p is the same as on p' . The following proof is similar to the first case. Therefore, we can obtain $E_\varphi^i < E_\varphi^{i*}$, which is also contradiction to the assumption that E_φ^{i*} is an optimal solution.

From above discussion, we can obtain that $U_{s_i}^{f*}$ is a tour on the line segment (b_{s_i}, s_i') , and both the starting point and ending point of $U_{s_i}^{f*}$ are b_{s_i} . \square

Theorem 2: We have $E_\varphi^i \leq E_\varphi^{i*} + \frac{r}{n \cdot v_f}$, where E_φ^i is obtained by PPSA.

Proof: According to definition of the PPS problem and Lemma 1, we should consider three cases as follows:

- (1) $HP_{s_i}^* \in (b_{s_i}, s_i')$;
- (2) There exists a $0 \leq t \leq 6n$ such that $HP_{s_i}^* \in (q_{t,0}, q_{t,\tau}) \setminus \{q_{t,0}\}$;
- (3) There exists a $0 \leq t \leq 6n$ such that $q_i^* \in (q_{t,0}, q_{t+1,0}) \setminus \{q_{t,0}, q_{t+1,0}\}$ and $HP_{s_i}^* \notin (b_{s_i}, s_i')$.

In the following, we will give the relationship between the time consumption of the optimal flight plan and the time consumption obtained by the PPSA algorithm for each of cases, and then obtain the performance ratio of the algorithm. For simplicity, we use V_U^* to represent the amount of transmission data from s_i to UAV when it flies on $U_{s_i}^*$.

In the first case, based on the Lemma 1, we know that there exists a $0 \leq t < 6n$ which satisfies

$$r - (t+1) \cdot \delta \leq d_{HP_{s_i}^*, s_i'} \leq r - t \cdot \delta, \quad (15)$$

as shown in Fig.6. then we can obtain

$$\begin{aligned} E_\varphi^{i*} &= \frac{2(r - d_{HP_{s_i}^*, s_i'})}{v_f} + \frac{2(V_i - V_U^*)}{W \log_2 \left(1 + \frac{\gamma_0}{(d_{HP_{s_i}^*, s_i'}^2 + h^2)^{\frac{\alpha}{2}}} \right)} \\ &\geq 2t \cdot \frac{\delta}{v_f} + \frac{2(V_i - V_U^*)}{W \log_2 \left(1 + \frac{\gamma_0}{((r - (t+1) \cdot \delta)^2 + h^2)^{\frac{\alpha}{2}}} \right)}. \end{aligned} \quad (16)$$

By taking $t+1$, let $V_U = \sum_{j=0}^t \frac{\delta}{v_f} W \log \left(1 + \frac{\gamma_0}{((r-j\delta)^2 + h^2)^{\frac{\alpha}{2}}} \right)$, which is the amount of data transmitted from s_i to UAV when it flies on the path $(b_{s_i}, q_{t+1,0}) \cup (q_{t+1,0}, b_{s_i})$ obtained by PPSA.

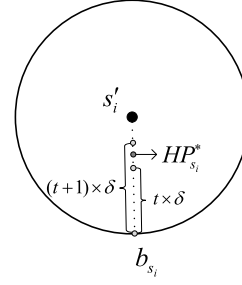


Fig. 6. An example t such that $r - (t+1) \cdot \delta < d_{HP_{s_i}^*, s_i'} \leq r - t \cdot \delta$.

Then, we have

$$V_U^* \leq V_U + \frac{\delta}{v_f} W \log \left(1 + \frac{\gamma_0}{((r - (t+1) \cdot \delta)^2 + h^2)^{\frac{\alpha}{2}}} \right). \quad (17)$$

Based on inequations (15)-(17) and algorithm PPSA, we can obtain

$$\begin{aligned} E_\varphi^i &\leq (t+1) \cdot \frac{2\delta}{v_f} + \frac{2(V_i - V_U)}{W \log_2 \left(1 + \frac{\gamma_0}{((r - (t+1) \cdot \delta)^2 + h^2)^{\frac{\alpha}{2}}} \right)} \\ &= (2t+4) \cdot \frac{\delta}{v_f} \\ &\quad + \frac{2(V_i - V_U - \frac{\delta}{v_f} W \log \left(1 + \frac{\gamma_0}{((r - (t+1) \cdot \delta)^2 + h^2)^{\frac{\alpha}{2}}} \right))}{W \log_2 \left(1 + \frac{\gamma_0}{((r - (t+1) \cdot \delta)^2 + h^2)^{\frac{\alpha}{2}}} \right)} \\ &\leq (2t+4) \cdot \frac{\delta}{v_f} + \frac{2(V_i - V_U^*)}{W \log_2 \left(1 + \frac{\gamma_0}{((r - (t+1) \cdot \delta)^2 + h^2)^{\frac{\alpha}{2}}} \right)} \\ &\leq E_\varphi^{i*} + \frac{4\delta}{v_f} < E_\varphi^{i*} + \frac{r}{n \cdot v_f}. \end{aligned}$$

In the second case, we can obtain that there exists a $1 \leq l < \tau$ which satisfies

$$l \cdot \eta \leq d_{HP_{s_i}^*, q_i^*} \leq (l+1) \cdot \eta. \quad (18)$$

By taking t , according to the inequation (18), we can obtain

$$\begin{aligned} E_\varphi^{i*} &= \frac{2d_{b_{s_i}, q_i^*}}{v_f} + \frac{2d_{q_i^*, HP_{s_i}^*}}{v_h} + \frac{2(V_i - V_U^*)}{W \log_2 \left(1 + \frac{\gamma_0}{d_{HP_{s_i}^*, s_i}^{\alpha}} \right)} \\ &\geq 2t \cdot \frac{\delta}{v_f} + 2l \cdot \frac{\eta}{v_h} + \frac{2(V_i - V_U^*)}{W \log_2 \left(1 + \frac{\gamma_0}{((r-t\delta)^2 + (h-(l+1)\eta)^2)^{\frac{\alpha}{2}}} \right)}. \end{aligned} \quad (19)$$

By taking $l+1$, let $V_U = \sum_{k=0}^t \frac{2\delta}{v_f} \cdot C_{q_{k,0}} + \sum_{j=1}^l \frac{2\eta}{v_h} \cdot C_{q_{t,j}}$ be the amount of data transmitted from s_i to UAV when it flies on the path $(b_{s_i}, q_{t,0}) \cup (q_{t,0}, q_{t,l+1}) \cup (q_{t,l+1}, q_{t,0}) \cup (q_{t,0}, b_{s_i})$ obtained by PPSA, where $C_{q_{k,0}} = \frac{1}{2} W \log_2 \left(1 + \frac{\gamma_0}{((r-k\delta)^2 + h^2)^{\frac{\alpha}{2}}} \right)$ for any $0 \leq k \leq t$ and $C_{q_{t,j}} = \frac{1}{2} W \log_2 \left(1 + \frac{\gamma_0}{((r-t\delta)^2 + (h-j\eta)^2)^{\frac{\alpha}{2}}} \right)$ for any $1 \leq j \leq l$. We can find that

$$V_U^* \leq V_U + \frac{\eta}{v_h} W \log \left(1 + \frac{\gamma_0}{((r-t\delta)^2 + (h-(l+1)\eta)^2)^{\frac{\alpha}{2}}} \right). \quad (20)$$

Since $\frac{\delta}{v_f} = \frac{\eta}{v_h}$, based on the algorithm PPSA and inequations (18)-(20), we can obtain

$$\begin{aligned} E_\phi^i &\leq 2t \cdot \frac{\delta}{v_f} + 2(l+1) \cdot \frac{\eta}{v_h} \\ &\quad + \frac{2(V_i - V_U)}{W \log_2 \left(1 + \frac{\gamma_0}{((r-t)\delta)^2 + (h-(l+1)\cdot\eta)^2} \frac{\alpha}{2}\right)} \\ &\leq 2t \cdot \frac{\delta}{v_f} + (2l+4) \cdot \frac{\eta}{v_h} \\ &\quad + \frac{2(V_i - V_U^*)}{W \log_2 \left(1 + \frac{\gamma_0}{((r-t)\delta)^2 + (h-(l+1)\cdot\eta)^2} \frac{\alpha}{2}\right)} \\ &\leq E_\phi^{i*} + \frac{4\eta}{v_h} < E_\phi^{i*} + \frac{r}{n \cdot v_f}. \end{aligned}$$

In the third case, we can obtain

$$r - (t+1) \cdot \delta < d_{q_i^*, s_i'} < r - t \cdot \delta, \quad (21)$$

Suppose $d_{q_{t+1,0}, q_i^*} = \varepsilon \cdot \delta$, where $0 < \varepsilon < 1$. Let q_i' be the projection point of q_i^* on $N(s_i')$. Then we divide (q_i^*, q_i') into τ parts, and $(q_{t+\varepsilon,0}, q_{t+\varepsilon,1}, \dots, q_{t+\varepsilon,\tau}) = (q_i^*, q_i')$, where $d_{q_{t+\varepsilon,l}, q_{t+\varepsilon,l+1}} = \eta$ for any $0 \leq l < \tau - 1$ and $d_{q_{t+\varepsilon,l}, q_{t+\varepsilon,l+1}} = h - h_0 - (\tau - 1) \cdot \eta$ for $l = \tau - 1$. Then, based on inequations (18) and (21), we can obtain

$$\begin{aligned} E_\phi^{i*} &= \frac{2d_{b_{s_i}, q_i^*}}{v_f} + \frac{2d_{q_i^*, HP_{s_i}^*}}{v_h} + \frac{2(V_i - V_U^*)}{W \log_2 \left(1 + \frac{\gamma_0}{d_{HP_{s_i}^*, s_i}^2}\right)} \\ &\geq \frac{2(t+\varepsilon) \cdot \delta}{v_f} + \frac{2l \cdot \eta}{v_h} \\ &\quad + \frac{2(V_i - V_U^*)}{W \log_2 \left(1 + \frac{\gamma_0}{((r-(t+\varepsilon)\delta)^2 + (h-(l+1)\cdot\eta)^2) \frac{\alpha}{2}}\right)} \\ &\geq 2t \cdot \frac{\delta}{v_f} + \frac{2l \cdot \eta}{v_h} \\ &\quad + \frac{2(V_i - V_U^*)}{W \log_2 \left(1 + \frac{\gamma_0}{((r-(t+1)\delta)^2 + (h-(l+1)\cdot\eta)^2) \frac{\alpha}{2}}\right)}. \quad (22) \end{aligned}$$

By taking $t+1$ and $l+1$, let $V_U = \sum_{k=0}^t \frac{2\delta}{v_f} \cdot C_{q_{k,0}} + \sum_{j=0}^l \frac{2\eta}{v_h} \cdot C_{q_{t+1,j}}$ be the amount of data transmitted from s_i to UAV when it flies on the path $(b_{s_i}, q_{t+1,0}) \cup (q_{t+1,0}, q_{t+1,l+1}) \cup (q_{t+1,l+1}, q_{t+1,0}) \cup (q_{t+1,0}, b_{s_i})$ obtained by PPSA, where $C_{q_{k,0}} = \frac{1}{2} W \log_2 \left(1 + \frac{\gamma_0}{((r-k)\delta)^2 + h^2} \frac{\alpha}{2}\right)$ for any $0 \leq k \leq t$ and $C_{q_{t+1,j}} = \frac{1}{2} W \log_2 \left(1 + \frac{\gamma_0}{((r-(t+1)\delta)^2 + (h-j\cdot\eta)^2) \frac{\alpha}{2}}\right)$ for any $0 \leq j \leq l$. We have

$$V_U^* \leq V_U + \frac{\eta}{v_h} W \log \left(1 + \frac{\gamma_0}{((r-(t+1)\delta)^2 + (h-(l+1)\cdot\eta)^2) \frac{\alpha}{2}}\right). \quad (23)$$

Based on inequations (21)-(23), we can obtain

$$\begin{aligned} E_\phi^i &\leq \frac{2(t+1)\delta}{v_f} + \frac{2(l+1)\eta}{v_h} \\ &\quad + \frac{2(V_i - V_U)}{\log_2 \left(1 + \frac{\gamma_0}{((r-(t+1)\delta)^2 + (h-(l+1)\cdot\eta)^2) \frac{\alpha}{2}}\right)} \end{aligned}$$

$$\begin{aligned} &\leq \frac{(2t+2)\delta}{v_f} + \frac{(2l+4)\eta}{v_h} \\ &\quad + \frac{2(V_i - V_U^*) \cdot \frac{1}{W}}{\log_2 \left(1 + \frac{\gamma_0}{((r-(t+1)\delta)^2 + (h-(l+1)\cdot\eta)^2) \frac{\alpha}{2}}\right)} \\ &\leq E_\phi^{i*} + \frac{2\delta}{v_f} + \frac{4\eta}{v_h} \leq E_\phi^{i*} + \frac{r}{n \cdot v_f}. \end{aligned}$$

From what has been discussed, we have $E_\phi^i \leq E_\phi^{i*} + \frac{r}{n \cdot v_f}$. \square

B. Algorithm for the FTPS Problem

In this subsection, we propose an approximation algorithm for solving the FTPS problem, which is called FTPSA. The objective of the algorithm is to find a flight plan $\Phi(U, H, T)$ of single UAV and

$$\text{Minimize } E_\Phi = \frac{L(U_f)}{v_f} + \frac{L(U_h)}{v_h} + t_{s_i},$$

where U_f and U_h represent the total horizontal flight path and total vertical flight path of UAV, respectively, and $U = U_f \cup U_h$.

The FTPSA consists of four steps. In the first step, we employ the $(1+\varepsilon)$ -approximation algorithm for the TSPN problem proposed in [23] to compute a tour U_f' for D , and obtain the order of the data collection areas in Θ visited by U_f' , which is denoted as $\Omega(s_{\rho_1}), \Omega(s_{\rho_2}), \dots, \Omega(s_{\rho_n})$, where $\Omega(s_{\rho_i})$ is the i -th data collection area visited by U_f' . In the second step, for each $\Omega(s_{\rho_i}) \in \Theta$, we compute the first intersection point $b_{s_{\rho_i}}$ between U_f' and $N(s_{\rho_i}')$. Let $b_{s_{\rho_i}}$ be the entry point of UAV to visit the data collection area $\Omega(s_{\rho_i})$. We compute the flight plan $\phi(U_{s_{\rho_i}}, HP_{s_{\rho_i}}, t_{s_{\rho_i}})$ and the time cost $E_\phi^{P_i}$ for UAV in $\Omega(s_{\rho_i})$ by executing the PPSA algorithm, where $U_{s_{\rho_i}}$ is comprised of the horizontal flight path $U_{s_{\rho_i}}^f$ and vertical flight path $U_{s_{\rho_i}}^h$ of UAV. Then we compute the projection point q_{ρ_i} of $HP_{s_{\rho_i}}$ on $N(s_{\rho_i}')$. Afterwards, we perform the operations $U_h = U_h \cup U_{s_{\rho_i}}^h$, $H = H \cup \{HP_{s_{\rho_i}}\}$ and $T = T \cup \{t_{s_{\rho_i}}\}$. In the third step, for any $1 \leq i \leq n$, we use the line segment $(q_{\rho_i}, q_{\rho_{i+1}})$ to be the horizontal flight path of UAV which is from q_{ρ_i} to $q_{\rho_{i+1}}$ (where $s_{\rho_{i+1}} = s_{\rho_1}$), and $U_f = U_f \cup (q_{\rho_i}, q_{\rho_{i+1}})$. Finally, the complete flight tour of UAV $U = U_f \cup U_h$ is derived, and then the flight plan $\Phi = \{U, H, T\}$ and the total time cost $E_\Phi = L(U_f)/v_f + L(U_h)/v_h + \sum_{t_{s_{\rho_i}} \in T} t_{s_{\rho_i}}$ of UAV are obtained. The pseudo-code of the algorithm is shown in Algorithm 2.

Suppose $\Phi(U^*, H^*, T^*)$ is an optimal flight plan of the UAV for the FTPS problem, where U^* is an optimal traveling tour of UAV, which consists of the optimal horizontal flight path U_f^* and vertical flight path U_h^* . H^* denotes an optimal set of hovering points of UAV on U^* in which for each $HP_{s_i}^* \in H^*$, there is a corresponding hovering time $t_{s_i}^* \in T^*$. We use E_Φ^* to denote the time consumption of UAV for the flight plan $\Phi(U^*, H^*, T^*)$.

Theorem 3: We have $E_\Phi \leq (2+\varepsilon) \cdot E_\Phi^ + \frac{r}{v_f}$, where E_Φ is obtained by using the FTPSA algorithm.*

Proof: Suppose U_{tp}^* is an optimal tour for the TSPN problem. Since U_f^* should visit all disks in D , we can obtain

Algorithm 2 FTPSA

Input: $S = \{s_1, s_2, \dots, s_n\}$, V_i for each $s_i \in S$, R , r ,
 $D = \{N(s'_1), N(s'_2), \dots, N(s'_n)\}$, W , γ_0 , h_0 ,
 $\Theta = \{\Omega(s_1), \Omega(s_2), \dots, \Omega(s_n)\}$, h , v_f , v_h , s_0

Output: A flight plan $\Phi(U, H, T)$ of UAV and E_Φ

- 1 Using the $(1 + \varepsilon)$ -approximation algorithm for the TSPN problem to compute a tour U'_f for D [23], and the order of data collection areas in Θ visited by U'_f , which is denoted as $\Omega(s_{\rho_1}), \Omega(s_{\rho_2}), \dots, \Omega(s_{\rho_n})$;
- 2 **for** each $\Omega(s_{\rho_i}) \in \Theta$ **do**
- 3 Compute the first intersection point $b_{s_{\rho_i}}$ between U'_f and $N(s'_{\rho_i})$, where U'_f is visited in counter clockwise order;
- 4 Compute the flight plan $\varphi(U_{s_{\rho_i}}, HP_{s_{\rho_i}}, t_{s_{\rho_i}})$ and the time cost $E_\varphi^{\rho_i}$ for UAV in the area $\Omega(s_{\rho_i})$ by executing the PPSA algorithm, where $U_{s_{\rho_i}} = U_{s_{\rho_i}}^f \cup U_{s_{\rho_i}}^h$, and compute the projection point q_{ρ_i} of $HP_{s_{\rho_i}}$ on $N(s'_{\rho_i})$;
- 5 $U_h = U_h \cup U_{s_{\rho_i}}^h$, $H = H \cup HP_{s_{\rho_i}}$, $T = T \cup t_{s_{\rho_i}}$;
- 6 **end**
- 7 **for** i from 0 to n **do**
- 8 Let $(q_{\rho_i}, q_{\rho_{i+1}})$ be the horizontal flight path of UAV which is from q_{ρ_i} to $q_{\rho_{i+1}}$, and $U_f = U_f \cup (q_{\rho_i}, q_{\rho_{i+1}})$;
- 9 **end**
- 10 $U = U_f \cup U_h$, $E_\Phi = L(U_f)/v_f + L(U_h)/v_h + \sum_{t_{s_{\rho_i}} \in T} t_{s_{\rho_i}}$;

that U'_f is a feasible solution for the TSPN problem. Thus, we have

$$L(U_{tp}^*) \leq L(U_f^*). \quad (24)$$

According to the algorithm for the TSPN problem, we can derive

$$L(U'_f) \leq (1 + \varepsilon) \cdot L(U_{tp}^*). \quad (25)$$

Based on the definition of FTPS problem, we can obtain

$$E_\Phi^* \geq \frac{L(U_f^*)}{v_f} + \frac{L(U_h^*)}{v_h}, \quad (26)$$

and

$$E_\Phi^* \geq \sum_{i=1}^n E_\varphi^{\rho_i^*}. \quad (27)$$

Since the shortest distance between any pair of points is the straight line for connecting them without any curves, we can get that for any $1 \leq i \leq n$,

$$d_{q_{\rho_i}, q_{\rho_{i+1}}} \leq \frac{1}{2} \cdot L(U_{s_{\rho_i}}^f) + \frac{1}{2} \cdot L(U_{s_{\rho_{i+1}}}^f) + L(P_{b_{s_{\rho_i}}, b_{s_{\rho_{i+1}}}}). \quad (28)$$

Based on the Theorem 2 and inequations (24)-(28), we can obtain

$$\begin{aligned} E_\Phi &= \frac{L(U_f)}{v_f} + \frac{L(U_h)}{v_h} + \sum_{t_{s_{\rho_i}} \in T} t_{s_{\rho_i}} \\ &= \frac{\sum_{i=1}^n d_{q_{\rho_i}, q_{\rho_{i+1}}}}{v_f} + \frac{L(U_h)}{v_h} + \sum_{t_{s_{\rho_i}} \in T} t_{s_{\rho_i}} \end{aligned}$$

$$\begin{aligned} &\leq \frac{L(U'_f)}{v_f} + \sum_{s_{\rho_i} \in S} \left(\frac{L(U_{s_{\rho_i}}^f)}{v_f} + \frac{L(U_{s_{\rho_i}}^h)}{v_h} + t_{s_{\rho_i}} \right) \\ &= \frac{L(U'_f)}{v_f} + \sum_{i=1}^n E_\varphi^{\rho_i} \leq \frac{(1 + \varepsilon) \cdot L(U_f^*)}{v_f} + \sum_{i=1}^n \left(E_\varphi^{\rho_i^*} + \frac{r}{n \cdot v_f} \right) \\ &\leq (2 + \varepsilon) \cdot E_\Phi^* + \frac{r}{v_f}. \end{aligned}$$

Hence, the theorem has been proved. \square

V. ALGORITHM FOR THE FTP PROBLEM

In this section, we propose an approximation algorithm, called FTPM, to solve the general FTP problem. The objective of the FTPM algorithm aims at finding a flight plan $\Phi(U, H, T)$ of m UAVs and

$$\text{Minimize } E_\Phi = \max_{1 \leq k \leq m} E_\Phi^k,$$

where E_Φ^k is the time cost of f_k .

The FTPM algorithm consists of five steps as follows.

In the first step, we compute the flight plan $\Phi(U_t, H_t, T_t)$ of the single UAV on Θ by executing the FTPSA algorithm, where U_t consists of the horizontal flight path U_t^f and vertical flight path U_t^h .

In the second step, for each $s_i \in S$, we create the virtual paths $P_{s_i^b, s_i^e}$ and $P_{s_i^1, s_i^2}$ to represent the horizontal flight path and vertical flight path of UAV with t_{s_i} and $\frac{d_{q_i, HP_{s_i}}}{v_h}$ flying time, respectively, i.e., $L(P_{s_i^b, s_i^e}) = v_f \cdot t_{s_i}$ and $L(P_{s_i^1, s_i^2}) = \frac{d_{q_i, HP_{s_i}}}{v_h} \cdot v_f$, where s_i^b and s_i^e are respectively the starting point and ending point of $P_{s_i^b, s_i^e}$, and s_i^1 and s_i^2 respectively denote the starting point and ending point of $P_{s_i^1, s_i^2}$. Then the paths $P_{s_i^b, s_i^e}$, $P_{s_i^1, s_i^2}$ and $P_{s_i^2, s_i^1}$ are added into Q , where Q is a set of virtual paths.

In the third step, we combine Q and U_t^f , and put the result into U_f , i.e., $U_f = U_t^f \cup Q$. Afterwards, we divide U_f into m paths P_1, P_2, \dots, P_m based on their counter-clockwise visiting sequence such that $L(P_k) = \frac{L(U_f)}{m}$ for any $1 \leq k \leq m$. Let c_k denote the connection point between P_k and P_{k+1} , where $1 \leq k \leq m-1$. For simplicity, we use c_k^b and c_k^e to represent the starting point and ending point of P_k , respectively. Initially, we have $c_1^b = c_m^e = s_0$, $c_k^e = c_k$ for any $1 \leq k \leq m-1$ and $c_k^b = c_{k-1}$ for any $2 \leq k \leq m$.

In the fourth step, for each $s_i \in S$ that is visited by the path P_k , we design the detailed flight plan of f_k in $\Omega(s_i)$ on the following two cases: $P_{s_i^b, s_i^e} \subset P_k$ and $c_k \in P_{s_i^b, s_i^e}$. In the former case, we let $HP_{s_i} \in H_t$ with the hovering time $L(P_{s_i^b, s_i^e})/v_f$ be the hovering point of f_k , and set $H_k = H_k \cup \{HP_{s_i}\}$, $T_k = T_k \cup \{L(P_{s_i^b, s_i^e})/v_f\}$ and $U_k^h = U_k^h \cup P_{s_i^1, s_i^2} \cup P_{s_i^2, s_i^1}$, where U_k^h represents the vertical flight path of f_k . If $\Omega(s_i)$ is the last data collection area visited by P_k , then the paths $P_{s_i^b, s_i^e}$ and $P_{s_i^e, c_k}$ are deleted from P_k , the path $P_{s_i^1, s_i^2}$ is added into P_k , and the end point c_k^e of P_k is changed to s_i^1 . Otherwise, if $\Omega(s_i)$ is the first data collection area visited by P_k , then the paths $P_{s_i^b, s_i^e}$ and P_{c_{k-1}, s_i^b} are deleted from P_k , the path $P_{s_i^2, s_i^1}$ is added into P_k , and the start point c_k^b of P_k is updated to s_i^1 . In the latter case, we let HP_{s_i} with the hovering time $L(P_{s_i^b, c_k})/v_f$ be the hovering point of f_k , and set $H_k = H_k \cup \{HP_{s_i}\}$, $T_k = T_k \cup \{L(P_{s_i^b, c_k})/v_f\}$.

Algorithm 3 FTPM

Input: $S = \{s_1, s_2, \dots, s_n\}$, V_i for each $s_i \in S$, r , R ,
 $F = \{f_1, f_2, \dots, f_m\}$, h , v_f , v_h , h_0 , W , γ_0 ,
 $\Theta = \{\Omega(s_1), \Omega(s_2), \dots, \Omega(s_n)\}$,
 $D = \{N(s'_1), N(s'_2), \dots, N(s'_n)\}$

Output: A flight plan $\Phi(U, H, T)$ for m UAVs and E_Φ

- 1 Compute the flight plan $\Phi(U_t, H_t, T_t)$ for the single UAV on Θ by executing Algorithm FTPSA;
- 2 **for** each $s_i \in S$ **do**
- 3 $P_{s_i^b, s_i^e} = t_{s_i} \cdot v_f$, $P_{s_i^1, s_i^2} = \frac{d_{q_i, HP_{s_i}}}{v_h} \cdot v_f$;
- 4 $Q = Q \cup P_{s_i^b, s_i^e} \cup P_{s_i^1, s_i^2} \cup P_{s_i^2, s_i^1}$;
- 5 **end**
- 6 $U_f = U_t^f \cup Q$, and divide U_f into m paths P_1, P_2, \dots, P_m such that $L(P_k) = \frac{L(U_f)}{m}$, and let c_k denote the connection point between P_k and P_{k+1} ;
- 7 **for** k from 1 to m **do**
- 8 **for** each $s_i \in S$ **do**
- 9 **if** $P_{s_i^b, s_i^e} \subset P_k$ **then**
- 10 $H_k = H_k \cup \{HP_{s_i}\}$, $T_k = T_k \cup \{\frac{L(P_{s_i^b, s_i^e})}{v_f}\}$;
- 11 $U_k^h = U_k^h \cup P_{s_i^1, s_i^2} \cup P_{s_i^2, s_i^1}$;
- 12 **if** $\Omega(s_i)$ is the last area visited by P_k **then**
- 13 $P_k = (P_k - P_{s_i^b, s_i^e} - P_{s_i^e, c_k}) \cup P_{s_i^2, s_i^1}$, $c_k^e = s_i^1$;
- 14 **end**
- 15 **if** $\Omega(s_i)$ is the first area visited by P_k **then**
- 16 $P_k = (P_k - P_{s_i^b, s_i^e} - P_{c_{k-1}, s_i^b}) \cup P_{s_i^2, s_i^1}$;
- 17 $c_k^b = s_i^1$;
- 18 **end**
- 19 **else**
- 20 **if** $c_k \in P_{s_i^b, s_i^e}$ **then**
- 21 $H_k = H_k \cup \{HP_{s_i}\}$, $T_k = T_k \cup \{\frac{L(P_{s_i^b, c_k})}{v_f}\}$;
- 22 $P_k = (P_k - P_{s_i^b, c_k}) \cup P_{s_i^2, s_i^1}$, $c_k^e = s_i^1$;
- 23 $s_i^b = c_k$, $U_k^h = U_k^h \cup P_{s_i^1, s_i^2} \cup P_{s_i^2, s_i^1}$;
- 24 **end**
- 25 **end**
- 26 $U_k = P_k \cup (s_0, c_k^b) \cup (c_k^e, s_0)$, $U_k^f = U_k - U_k^h$;
- 27 $E_\Phi^k = \frac{L(U_k^f)}{v_f} + \frac{L(U_k^h)}{v_h} + \sum_{t_{s_i}^k \in T_k} t_{s_i}^k$, $U = U \cup U_k$;
- 28 **end**
- 29 $\Phi = \{U, H, T\}$, $E_\Phi = \max_{1 \leq k \leq m} E_\Phi^k$;

Afterwards, we delete the path $P_{s_i^b, c_k}$ from P_k and add the path $P_{s_i^2, s_i^1}$ into P_k . Then the ending point c_k^e of P_k is set to s_i^1 and the starting point of path $P_{s_i^b, s_i^e}$ is changed to c_k . This is because when the amount of sensory data carried by s_i is very large, we may need several UAVs to collect its data simultaneously. Afterwards, we add the paths $P_{s_i^1, s_i^2}$ and $P_{s_i^2, s_i^1}$ into the path U_k^h . After completing this step, for any $f_k \in F$, the flight plan $\phi(P_k, H_k, T_k)$ is obtained.

Finally, for any $f_k \in F$, we construct the flight tour of f_k by combining P_k , (s_0, c_k^b) and (c_k^e, s_0) , i.e., $U_k = P_k \cup (s_0, c_k^b) \cup (c_k^e, s_0)$, and its horizontal flight time is $U_k^f = U_k - U_k^h$.

Therefore, we can calculate the time cost of f_k as $E_\Phi^k = L(U_k^f)/v_f + L(U_k^h)/v_h + \sum_{t_{s_i}^k \in T_k} t_{s_i}^k$. Consequently, the time cost $E_\Phi = \max_{1 \leq k \leq m} E_\Phi^k$ is obtained. The pseudo-code of the FTPM algorithm is given in Algorithm 3.

Next, we will analyze the performance of the FTPM algorithm. Suppose $\Phi(U^*, H^*, T^*)$ is an optimal flight plan of m UAVs for the FTP problem, where $U^* = \{U_1^*, U_2^*, \dots, U_m^*\}$, $H^* = \{H_1^*, H_2^*, \dots, H_m^*\}$, $T^* = \{T_1^*, T_2^*, \dots, T_m^*\}$ and let E_Φ^* denote the time cost of the flight plan $\Phi(U^*, H^*, T^*)$. For any $1 \leq k \leq m$, let $U_k^* = U_k^{f*} \cup U_k^{h*}$, where U_k^{f*} and U_k^{h*} denote the optimal horizontal flight path and vertical flight path of f_k , respectively. Let $U_j^* = \{U_1^{f*}, U_2^{f*}, \dots, U_m^{f*}\}$.

Theorem 4: We have $E_\Phi \leq (3 + \varepsilon) \cdot E_\Phi^* + \frac{2r}{v_f}$, where E_Φ is obtained by the FTPM algorithm.

Proof: Suppose $U_c^{f*} = \bigcup_{k=1}^m U_k^{f*}$ is the union of all tours in U_j^* . Since all tours in U_j^* can jointly visit all disks in D and converge on s_0 , we can find that U_c^{f*} is a feasible solution for the TSPN problem. Thus, we have $L(U_c^{f*}) \geq L(U_{tp}^*)$. Let $L(U_j^*) = \max\{L(U_k^{f*}) | U_k^{f*} \in U_j^*\}$. Then, we can obtain

$$L(U_j^*) \geq \frac{1}{m} \cdot L(U_c^{f*}) \geq \frac{1}{m} \cdot L(U_{tp}^*). \quad (29)$$

According to the definition of FTP problem, we can get

$$E_\Phi^* \geq \frac{L(U_j^*)}{v_f}, \quad (30)$$

and

$$E_\Phi^* \geq \frac{1}{m} \cdot \sum_{s_i \in S} E_\Phi^{i*}. \quad (31)$$

Based on the FTPM algorithm, we can obtain for each $1 \leq k \leq m$, both the starting point c_k^b and ending point c_k^e of P_k are located in the disks in D . Suppose c_k^b is located in $N(s'_i)$ and c_k^e is in the disk $N(s'_j)$. Then we can obtain

$$L(s_0, c_k^b) \leq L(s_0, s'_i) + r, \quad (32)$$

and

$$L(c_k^e, s_0) \leq L(s_0, s'_j) + r. \quad (33)$$

Since for any data collection area $\Omega(s_i) \in \Theta$, it should be visited by one of UAVs in F and the UAV should arrive at $\Omega(s_i)$ from s_0 and go back to s_0 . Therefore, we have

$$E_\Phi^* \geq 2 \max_{\Omega(s_i) \in \Theta} \frac{L(s_0, s'_i) - r}{v_f}. \quad (34)$$

Based on Theorem 2 and the inequations (29)-(34), for any $f_k \in F$ and $m \geq 2$, we can obtain

$$\begin{aligned} E_\Phi^k &= \frac{L(U_f^k)}{v_f} + \frac{L(U_h^k)}{v_h} + \sum_{t_{s_i}^k \in T_k} t_{s_i}^k \\ &= \frac{L(P_k)}{v_f} + \frac{L(s_0, c_k^b)}{v_f} + \frac{L(c_k^e, s_0)}{v_f} + \sum_{t_{s_i}^k \in T_k} t_{s_i}^k \\ &\leq \frac{1}{m} \left(\frac{L(U_t^f)}{v_f} + \sum_{s_i \in S} E_\Phi^{i*} \right) + \frac{L(s_0, c_k^b)}{v_f} + \frac{L(c_k^e, s_0)}{v_f} \\ &\leq \frac{1}{m} \left((1 + \varepsilon) \cdot \frac{L(U_{tp}^*)}{v_f} + \sum_{s_i \in S} (E_\Phi^{i*} + \frac{r}{n \cdot v_f}) \right) + E_\Phi^* + \frac{2r}{v_f} \end{aligned}$$

$$\begin{aligned} &\leq \frac{1}{m}(1+\varepsilon)\frac{L(U_f^*)}{v_f} + \frac{1}{m} \cdot \sum_{s_i \in S} E_\phi^{i*} + \frac{1}{m} \cdot \frac{r}{v_f} + E_\Phi^* + \frac{2r}{v_f} \\ &\leq (3+\varepsilon) \cdot E_\Phi^* + \frac{3r}{v_f}. \end{aligned}$$

Consequently, we have

$$E_\Phi = \max_{1 \leq k \leq m} E_\phi^k \leq (3+\varepsilon) \cdot E_\Phi^* + \frac{3r}{v_f}.$$

Hence, the theorem has been proved. \square

According to Theorem 4, we can obtain that the FTPM have the constant approximation ratio for the FTP problem. However, in the case of steep terrain, such as in a mountainous environment, since sensors are deployed in the different altitudes, the data collection areas of sensors are different in size when the UAVs fly horizontally with fixed altitude. Based on the proposed algorithm for the FTP problem, we can firstly design traveling paths of UAVs for visiting all data collection areas in various sizes. If UAVs need to fly above and outside the transmission ranges of sensors due to the complex terrain, we can use the the projection points of the sensors on the flight plane of UAVs to be the starting points for visiting their data collection areas. Then for each sensor in the network, we find the optimal traveling paths of the visited UAVs by changing vertical cruising height to obtain the best tradeoff between traveling cost and hovering consumption of UAVs.

VI. SIMULATION RESULTS

In this section, we evaluate the average performance of the approximation algorithm FTPM through simulations on several key performance metrics under different settings. We implement the code using MATLAB 2013. In the simulations, sensors are deployed in a 2000 m \times 2000 m detection area, the reference SNR at transmission distance 1 m is set to $\gamma_0 = 80$ dB and the path loss exponent is set to $\alpha = 3$. For each parameter setting, we create 100 instances, execute the simulations, and obtain the average results.

Given an FTP instance, we compute the lower bound of the time cost of any feasible solution for the FTP problem as follows: (a) A minimum spanning tree T_r of D is computed, and we let U_D^* denote an optimal tour to visit all disks in D , where disks in D are referred as points. (b) The time cost E_ϕ^i of UAV for each $\Omega(s_i) \in \Theta$ is computed by algorithm PPSA. (c) The lower bound of the solution for the FTP problem is equal to $\frac{1}{m} \cdot (\frac{L(T_r)}{v_f} + \sum_{\Omega(s_i) \in \Theta} E_\phi^i - \frac{r}{v_f})$, since $E_\Phi^* \geq \frac{1}{m} \cdot (\frac{L(U_D^*)}{v_f} + \sum_{\Omega(s_i) \in \Theta} E_\phi^{i*}) \geq \frac{1}{m} \cdot (\frac{L(T_r)}{v_f} + \sum_{\Omega(s_i) \in \Theta} E_\phi^i - \frac{r}{v_f})$ based on Theorem 2. In the following, we use $E_{max} = \max\{E_\phi^k | f_k \in F\}$ and $E_{min} = \min\{E_\phi^k | f_k \in F\}$ to denote the maximum time cost and the minimum time cost of m UAVs obtained by the FTPM algorithm, respectively. Then we evaluate how the network configurations, such as the number of sensors n , the number of UAVs m , the Bandwidth W , the amount of data V_i carried by each sensor $s_i \in S$, the data transmission range R , the horizontal flight speed v_f , the vertical flight speed v_h and horizontal flight altitude h , impact on the performance of FTPM algorithm by comparing E_{max} , E_{min} with Lower Bound.

In Fig. 7, we give the performance of FTPM when we set $R = 100$ m, $h = 60$ m, $h_0 = 10$ m, $W = 2$ MB/s, $v_f = 10$ m/s,

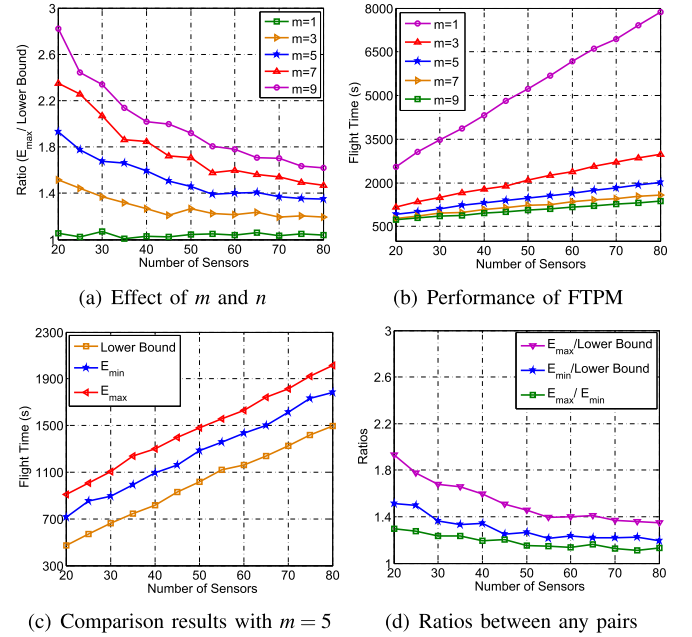


Fig. 7. Simulations by varying n from 20 to 80 under different m .

$v_h = 2$ m/s and use the interval $[1, 3]$ MB to pick a uniformly distributed random data size V_i for each sensor $s_i \in S$, and vary m to 1, 3, 5, 7, 9 and n from 20 to 80 increased by 5. In Fig. 7(a), we compare the performance of FTPM against the lower bound in terms of the ratio of E_{max} to the Lower Bound. It is observed that the ratio becomes higher as m grows, and that the performance gap is getting smaller and stabilized with an increase in the number of sensors, since the total time consumption for each UAV in data collection areas of sensors increases as n grows and the time cost of the lower bound in each data collection area got by PPSA is infinitely close to the optimal solution for the PPS problem. We also find that the ratio of E_{max} to the Lower Bound is always less than 3, which verifies the effectiveness of the FTPM algorithm, and that FTPM performs reasonably well in a larger network. Fig. 7(b) is to illustrate the impact of the number of sensors on the time cost of UAV. We can find that E_{max} increases with the increasing of the number of sensors since both the hovering time and traveling time of UAVs are increased as the number of sensors grows. We can also observe that the performance gap is becoming smaller with increasing m . This is because the traveling time of UAVs becomes the main part of the time cost of UAVs while the traveling distance of each UAV does not increase very much as m grows. In Fig. 7(c), we give the comparison of E_{max} , E_{min} and Lower Bound with $m=5$. It shows that all three increase as the number of sensors increases, which can guarantee the ratios in Fig. 7(a). We can also observe that the performance gap between E_{max} and E_{min} got by the algorithm FTPM is very small and stabilized, which can prove the validity of the algorithm. Fig. 7(d) illustrates the ratios between any pairs of E_{max} , E_{min} and Lower Bound when $m=5$. We can find the ratios $E_{max}/LowerBound$, $E_{min}/LowerBound$ and E_{max}/E_{min} decrease with the increasing of n since both the hovering time and traveling time of UAVs are increased as n grows.

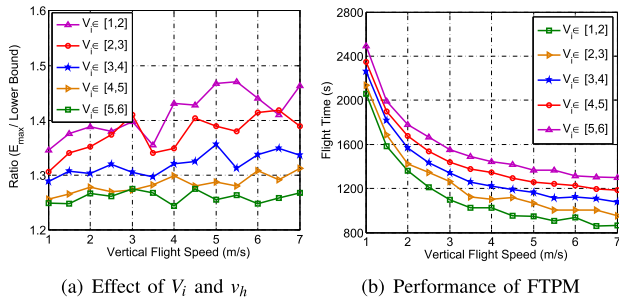


Fig. 8. Simulations through changing v_h from 1 m/s to 7 m/s under different V_i .

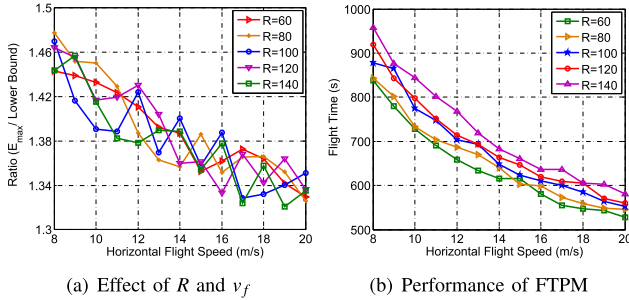


Fig. 9. Simulations through changing v_f from 8 m/s to 20 m/s under different R .

Fig. 8 illustrates the performance of FTPM when we set $n = 60$, $R = 100$ m, $h = 60$ m, $h_0 = 10$ m, $v_f = 15$ m/s, $m = 5$ and randomly pick V_i from the intervals [1,2], [2,3], [3,4], [4,5], and [5,6] MB, respectively and change v_h from 1 m/s to 7 m/s. Fig. 8(a) gives the changing trend of the ratio of E_{max} to the lower bound as v_h grows. It is observed that the ratio of E_{max} to the Lower Bound tends to balance with the increasing of v_h . This is because although the vertical flight time of UAV decreases as v_h grows, the traveling time outside of data collection areas becomes the major part of E_{max} , which makes the ratio of E_{max} to lower bound remain unchanged. We can find the ratio of E_{max} to the Lower Bound is always less than 1.5, which can prove the validity of the algorithm. We also find that the ratio decreases with increasing V_i for each sensor since both the hovering times of E_{max} and Lower Bound increase as the amount of data carried by sensors grows. Fig. 8(b) shows that E_{max} decreases with the increasing of v_h since UAVs need less vertical flight time to arrive the hovering point in each data collection area for gathering data from sensor.

In Fig. 9, we use the interval [1,3] MB to pick a uniformly distributed random V_i for each sensor $s_i \in S$ and set $n = 30$, $h = 50$ m, $W = 2$ MB/s, $m = 3$ and $R = 60, 80, 100, 120, 140$ m, and change v_f from 8 to 20 m/s. Fig. 9(a) shows that the ratio of E_{max} to the Lower Bound decreases with increasing v_f . This is because the hovering time part of both E_{max} and Lower Bound is unchanged while the traveling time of them decreases as v_f grows. We also observe that the ratio of E_{max} to Lower Bound becomes larger as R increases, since the traveling time of both E_{max} and the Lower Bound increases with increasing R but the hovering time of them is unchanged and becomes the main time cost of UAVs. Fig. 9(b) shows that the time cost of UAVs decreases as v_f grows since the total traveling time of UAV decreases with the increasing of v_f . We also find the time consumption of UAV decreases as R

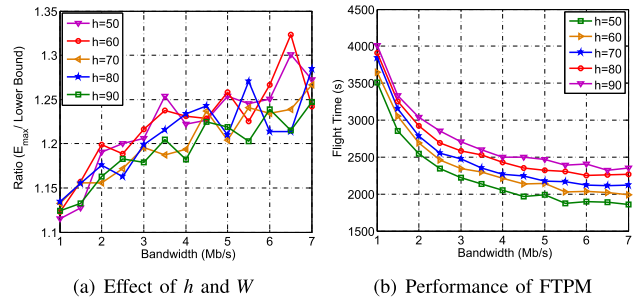


Fig. 10. Simulations through varying W from 1 Mb/s to 7 Mb/s under different h .

decreases. This is because that the data transmission rate from sensors to UAV raises with the decreasing of R , which leads to descent in the total time consumption of UAV.

Fig. 10 illustrates the performance of FTPM when we set $n = 60$, $R = 100$ m, $m = 3$, $v_f = 10$ m/s, $v_h = 3$ m/s, $h_0 = 10$ m, randomly pick V_i from the interval [5, 6] Mb and $h = 50, 60, 70, 80, 90$, and change W from 1Mb/s to 7Mb/s. Fig. 10(a) gives the changing trend of the ratio of E_{max} to the Lower Bound. It is observed that the ratio decreases with the increasing of W . This is because as W increases, the proportion of the horizontal flight time outside of data collection areas to E_{max} increases while the proportion of the horizontal flight time outside of data collection areas of Lower Bound, $\frac{L(T_r)}{v_f}$ is unchanged. We also find the ratio of E_{max} to Lower Bound remains stable as h increases, since both the horizontal flight time and vertical flight time of UAVs decreases, which can keep their values unchanged. Fig. 10(b) shows that E_{max} decreases with the increasing of W since UAVs need less data transmission time to collect data from sensors.

VII. CONCLUSION

In this paper, we identify the Fine-grained Trajectory Plan for multi-UAVs (FTP) problem, which focuses on finding the fine-grained trajectory plans for m UAVs. The objective of the problem is to minimize the maximum time cost of UAVs such that all sensory data carried by sensors in WSN is collected and transported to the base station. Then we prove that the FTP problem is NP-hard. Afterwards, we first investigate a special case of FTP problem where $m = 1$, called FTPS. Then we propose an approximation algorithm FTPSA for solving the FTPS problem. Based on the FTPSA algorithm, we present an approximation algorithm FTPM to design a fine-grained flight plan for each of m UAVs, which not only gives the flight paths of multiple UAVs but also provides the detailed hovering and traveling plans of UAVs. According to the theoretical analysis and simulations, we can verify that the proposed algorithms have great performance.

REFERENCES

- [1] J. Li, S. Cheng, Z. Cai, J. Yu, C. Wang, and Y. Li, "Approximate holistic aggregation in wireless sensor networks," *ACM Trans. Sensor Netw.*, vol. 13, no. 2, p. 11, Aug. 2017.
- [2] C. Luo, J. Yu, D. Li, H. Chen, Y. Hong, and L. Ni, "A novel distributed algorithm for constructing virtual backbones in wireless sensor networks," *Comput. Netw.*, vol. 146, pp. 104–114, Dec. 2018.
- [3] P. Bupe, R. Haddad, and F. Rios-Gutierrez, "Relief and emergency communication network based on an autonomous decentralized UAV clustering network," in *Proc. SoutheastCon*, Apr. 2015, pp. 1–8.

- [4] Y. Zeng, R. Zhang, and T. J. Lim, "Wireless communications with unmanned aerial vehicles: Opportunities and challenges," *IEEE Commun. Mag.*, vol. 54, no. 5, pp. 36–42, May 2016.
- [5] M. Erdelj, E. Natalizio, K. R. Chowdhury, and I. F. Akyildiz, "Help from the sky: Leveraging UAVs for disaster management," *IEEE Pervas. Comput.*, vol. 16, no. 1, pp. 24–32, Jan. 2017.
- [6] D. Kim, L. Xue, D. Li, Y. Zhu, W. Wang, and A. O. Tokuta, "On theoretical trajectory planning of multiple drones to minimize latency in search-and-reconnaissance operations," *IEEE Trans. Mobile Comput.*, vol. 16, no. 11, pp. 3156–3166, Nov. 2017.
- [7] J. Gong, T.-H. Chang, C. Shen, and X. Chen, "Flight time minimization of UAV for data collection over wireless sensor networks," *IEEE J. Sel. Areas Commun.*, vol. 36, no. 9, pp. 1942–1954, Sep. 2018.
- [8] M. B. Ghorbel, D. Rodriguez-Duarte, H. Ghazzai, M. J. Hossain, and H. Menouar, "Joint position and travel path optimization for energy efficient wireless data gathering using unmanned aerial vehicles," *IEEE Trans. Veh. Technol.*, vol. 68, no. 3, pp. 2165–2175, Mar. 2019.
- [9] C. Luo, Y. Wang, Y. Hong, W. Chen, X. Ding, Y. Zhu, and D. Li, "Minimizing data collection latency with unmanned aerial vehicle in wireless sensor networks," *J. Combinat. Optim.*, vol. 38, pp. 1–24, Jul. 2019.
- [10] D. Bhaduria and V. Isler, "Data gathering tours for mobile robots," in *Proc. IEEE/RSJ Int. Conf. Intell. Robots Syst.*, Oct. 2009, pp. 3868–3873.
- [11] H. Huang, A. V. Savkin, and C. Huang, "I-UMDPC: The improved-unusual message delivery path construction for wireless sensor networks with mobile sinks," *IEEE Internet Things J.*, vol. 4, no. 5, pp. 1528–1536, Oct. 2017.
- [12] S. K. Singh, P. Kumar, and J. P. Singh, "An energy efficient protocol to mitigate hot spot problem using unequal clustering in WSN," *Wireless Pers. Commun.*, vol. 101, no. 2, pp. 799–827, Jul. 2018.
- [13] N. Kumar and D. Dash, "Flow based efficient data gathering in wireless sensor network using path-constrained mobile sink," *J. Ambient Intell. Humanized Comput.*, vol. 11, pp. 1163–1175, Feb. 2019.
- [14] Y. Zeng and R. Zhang, "Energy-efficient UAV communication with trajectory optimization," *IEEE Trans. Wireless Commun.*, vol. 16, no. 6, pp. 3747–3760, Jun. 2017.
- [15] S. Liu, Z. Wei, Z. Guo, X. Yuan, and Z. Feng, "Performance analysis of UAVs assisted data collection in wireless sensor network," in *Proc. IEEE 87th Veh. Technol. Conf. (VTC Spring)*, Jun. 2018, pp. 1–5.
- [16] H. Binol, E. Bulut, K. Akkaya, and I. Guvenc, "Time optimal multi-UAV path planning for gathering its data from roadside units," in *Proc. IEEE 88th Veh. Technol. Conf. (VTC-Fall)*, Aug. 2018, pp. 1–5.
- [17] B. Liu and H. Zhu, "Energy-effective data gathering for UAV-aided wireless sensor networks," *Sensors*, vol. 19, no. 11, p. 2506, May 2019.
- [18] Y. Guo, S. Yin, and J. Hao, "Resource allocation and 3-D trajectory design in wireless networks assisted by rechargeable UAV," *IEEE Wireless Commun. Lett.*, vol. 8, no. 3, pp. 781–784, Jun. 2019.
- [19] J.-S. Lee and K.-H. Yu, "Optimal path planning of solar-powered UAV using gravitational potential energy," *IEEE Trans. Aerosp. Electron. Syst.*, vol. 53, no. 3, pp. 1442–1451, Jun. 2017.
- [20] E. Natalizio, N. R. Zema, L. Di Puglia Pugliese, and F. Guerriero, "Download and fly: An online solution for the UAV 3D trajectory planning problem in smart cities," in *Proc. 9th ACM Symp. Design Anal. Intell. Veh. Netw. Appl. (DIVANet)*, 2019, pp. 49–56.
- [21] P. B. Sujit, D. E. Lucani, and J. B. Sousa, "Joint route planning for UAV and sensor network for data retrieval," in *Proc. IEEE Int. Syst. Conf. (SysCon)*, Apr. 2013, pp. 688–692.
- [22] C. H. Papadimitriou, "The Euclidean travelling salesman problem is NP-complete," *Theor. Comput. Sci.*, vol. 4, no. 3, pp. 237–244, Jun. 1977.
- [23] A. Dumitrescu and J. S. B. Mitchell, "Approximation algorithms for TSP with neighborhoods in the plane," *J. Algorithms*, vol. 48, no. 1, pp. 135–159, Aug. 2003.



Chuanwen Luo received the Ph.D. degree from the School of Information, Renmin University of China, Beijing, China, in 2020. He is currently working as an Assistant Professor with the School of Information Science and Technology, Beijing Forestry University, Beijing. He was a Visiting Scholar with the Department of Computer Science, The University of Texas at Dallas, in 2019. His research interests include various topics in the application of wireless networks, ad hoc and sensor networks, and algorithm design and analysis.



Meghana N. Satpute received the M.E. degree in computer engineering from the University of Pune, Pune, India, and the Ph.D. degree in computer science from The University of Texas at Dallas. She is currently an Assistant Professor with the Department of Computer Sciences, The University of Texas at Dallas. Her current research interests include applying combinatorial optimization algorithms for solving natural language processing problems and wireless communication problems.



Deying Li received the B.S. and M.S. degrees in mathematics from Central China Normal University, Wuhan, in 1985 and 1988, respectively, and the Ph.D. degree in computer science from the City University of Hong Kong in 2004. She is currently a Professor with the Department of Computer Science, Renmin University of China. Her research interests include wireless networks, ad hoc and sensor networks, distributed network systems, social networks, and algorithm design.



Yongcai Wang (Member, IEEE) received the B.S. and Ph.D. degrees from the Department of Automation Sciences and Engineering, Tsinghua University, in 2001 and 2006, respectively. He worked as an Associate Researcher with NEC Laboratories China, from 2007 to 2009. He was a Research Scientist with the Institute for Interdisciplinary Information Sciences, Tsinghua University, from 2009 to 2015. He was a Visiting Scholar with the Department of Electronic and Computer Engineering, Cornell University, in 2015. He is currently an Associate Professor with the Department of Computer Science, Renmin University of China. His current research interests include network localization algorithms, simultaneously locating and mapping algorithms, combinatorial optimization, and applications.



Wenping Chen received the B.E. and M.E. degrees from the Department of Computer Science and Technology, Xi'an Jiaotong University, in 1997 and 2000, respectively, and the Ph.D. degree from the Department of Computer Science and Technology, Tsinghua University, in 2003. She is currently working as an Assistant Professor with the Department of Computer Science, Renmin University of China. Her current research interests include mobile computing, wireless ad hoc networks, and social computing.



Weili Wu (Senior Member, IEEE) received the M.S. and Ph.D. degrees from the Department of Computer Science, University of Minnesota, Minneapolis, MN, USA, in 1998 and 2002, respectively. She is currently a Full Professor with the Department of Computer Science, The University of Texas at Dallas, Richardson, TX, USA. Her research interests include the design and analysis of algorithms for optimization problems that occur in wireless networking environments and various database systems.